Journal of Applied Meteorology and Climatology

Evaluation of Modeled Lake Breezes Using an Enhanced Observational Network in Southern Ontario: Case Studies

--Manuscript Draft--

Manuscript Number:	JAMC-D-17-0231
Full Title:	Evaluation of Modeled Lake Breezes Using an Enhanced Observational Network in Southern Ontario: Case Studies
Article Type:	Article
Order of Authors:	Armin Dehghan
	Zen Mariani
	Sylvie Leroyer
	David Sills
	Stephane Belair
	Paul Joe
Manuscript Classifications:	3.328: Sea breezes; 5.116: Remote sensing; 5.140: Surface observations; 8.116: Model evaluation/performance
Abstract:	Canadian Global Environmental Multiscale (GEM) numerical model output was compared to the meteorological data from an enhanced observational network in order to investigate the model's ability to predict Lake Ontario lake breezes and their characteristics for two cases in the Greater Toronto Area (GTA) - one where the large-scale wind opposed the lake breeze and one where it was in the same direction as the lake breeze. The enhanced observational network of surface meteorological stations, a C-band radar and two Doppler wind lidars were deployed among other sensors during the 2015 Pan/Parapan American Games in Toronto. The GEM model was run for three nested domains with grid spacings of 2.5, 1 and 0.25 km. Comparisons between the model predictions and ground-based observations showed that the model successfully predicted lake breezes for the two events. The results indicated that using GEM 1 and 0.25 km increased the forecast accuracy of the lake-breeze location, updraft intensity and depth. The accuracy of the modeled lake breeze timing was approximately ±90 minutes. The model under-predicted the surface cooling caused by the lake breeze. The GEM 0.25 km model significantly improved the temperature forecast accuracy during the lake-breeze circulations, reducing the bias by up to 72%, but it mainly under-predicted the moisture and over-predicted the surface wind speed. Root Mean Square Errors of wind direction forecasts were generally high due to large biases and high variability of errors.

Powered by Editorial Manager® and ProduXion Manager® from Aries Systems Corporation

Response to Reviewers
Click here to download Response to Reviewers Authorsresponse_final.docx

Authors' Response

The authors thank the reviewers and the editor. We believe that their comments and constructive suggestions have improved our manuscript. We have responded to all the comments in red italics.

Response to Editor

The two lake breeze case studies present an interesting evaluation of how well such events can be simulated by the GEM model. I concur with the reviewers, however, that the paper requires additional work to more clearly support your interpretation and analysis. It will be especially important to provide additional synoptic or mesoscale context for these two cases, to justify the choice of the 9 August event, and to ensure that the figures and tables adequately support the interpretation presented in text.

We have undertaken additional work and modified the manuscript to justify the choice of the 9 August event.

Response to Reviewer 1

Major comments:

Particularly in Fig. 6c, the checkerboard pattern in the earlier part of the time frame makes me suspect numerical instability. There is little indication of physical distance on the x-axis of this figure, but it would be useful to know whether centers of upward motion happen at intervals of 2 grid cells. Also, it might be useful to know what time steps were used for the different model resolutions.

We believe this is not a numerical instability. The predicted vertical velocity was examined in the region for different hours and this was not the case. These are resolved circulations (~ 4-8 × grid spacing) by the model. The L1B, L1E and A2T on the x-axis are located approximately at 6, 15 and 28 km from the shore. The bands of upward motion could be narrow (within 2 grid cells) though the distance between the bands are often *> 4-8 × grid spacing which shows that the model resolved the turbulent structures.The time steps for different resolutions are given in Table 2.*

Lines 253-254: How do you resolve a distance of 2.2 km using a 2.5 km grid? Lines 258 and 262 show averages of 2.3 and 2.4, respectively, indicating to me that most snapshots had a value of 2.5 km, while for a small minority, it snapped to 0. If this is the case, you should probably say so.

The inland penetration of the predicted lake-breeze front was estimated using interpolation of vertical and horizontal velocity for 100 points along the cross-section (shore-A2T). Since the

distance between the shore and A2T along the cross-section is 28 km, the values are given to the nearest 0.28 km due to the density of points used along the transect but it is realized that the uncertainty is larger than that, depending on the grid size used. This has been added to the text (lines 232-237).

Minor comments:

It might be useful to have a very brief description of any special observing systems that were deployed for the previous studies described in the introduction, for later comparison with your observing systems.

We have added a description of the lidar, mesonet and radar used in Mariani et al. (2017) to Section 2. The measurements from other works in the introduction were not compared to our measurements, therefore we have not included the description of their observing systems.

Section 2b: How far inland does the mesonet extend?

It extends to Lake Simcoe; ~ 100 km from the Lake Ontario shorelake.

Line 131: Do you mean more specifically which direction a roof is facing relative to the Sun? I think you should say this.

No, we are referring to wind measurements affecting by the location of the sensors on the rooftop.

Lines 157-159: I don't think you have given an adequate description of the turbulent flux scheme. You have only given references for the way that roughness lengths are calculated. After that, you also need equations (or references that contain the equations) for the fluxes based on roughness length, wind speed, vertical temperature/mixing ratio gradient, and in some formulations, other things.

We have added references (Belair et al. 2003; Leroyer et al. 2010) to the text to include more information on the turbulent flux scheme (lines 160-162).

Line 161: If you are capitalizing "Biosphere" and "Atmosphere", also capitalize "Interaction" and "Surface".

Done.

Line 175: I wonder whether increase in dew point is really a necessary condition. If you have a very strong contrast between colder water and warmer land, the incoming lake breeze can be drier. Fig. 3d looks like it has higher dew points inland from the front in the western part, maybe slightly opposite of that in the central part, and little gradient right at the front in the eastern part.

*It is not a necessary condition. The passage of a lake-breeze front **may** be accompanied by sharp changes in temperature, dew point and wind speed (lines 181-183).*

Don't feel badly about this, as I correct hyphenation on nearly every paper I review, whether the authors are native English speakers or not. See rule 1 on this page: http://www.grammarbook.com/punctuation/hyphens.asp. "Lake breeze" has the noun "lake" acting like an adjective to modify the noun "breeze". "Lake-breeze front" has those two words tied together by a hyphen to form a compound adjective, modifying the noun "front". If "lake breeze" or "lake breezes" is not followed by a noun that it modifies, as on line 186, do not use a hyphen. I personally feel like, in this case, even if "front" is included, the hyphen is optional.

It has been corrected.

I am confused by the description of north-easterly flow as opposing (lines 181-182) and east/north-easterly flow as non-opposing (line 184). How different are they?

This has changed to northerly/north-north-easterly for opposing wind and easterly/east-north-easterly for non-opposing wind (lines 194-197).

The problem in the previous comment is made worse by the very tiny size of the wind vectors in Figs. 3b and 4b, such that I can't see which direction they are pointing. Make them bigger and less dense.

We have made the wind vectors less dense but we did not change the wind vector sizes since they will overlap.

In Fig. 5, do the white dots indicate the penetration of the front as given by mesonet analysis or some other source? Please specify in the caption.

Yes, they do. This has been added to the Caption.

Fig. 7's caption says, "North is on the right." This is also true for Figs. 5 and 6. I'm not entirely sure that it is necessary to say that, but if you do, say it for Fig. 5.

This has been removed.

Line 257 and elsewhere: "Average differences" can be interpreted in at least two ways. One way, the bias, is to simply add up the values of the discrepancies and divide by the number of data points. Another, mean absolute error, has an absolute value operation done on all of the data before adding them. If all values are positive, these statistics will be the same; if all are negative, the bias will be the negative of the MAE. So part of the question here is that line 256 says "generally underestimated". Could you truthfully say that "the distance of penetration from observations is always greater than or equal to the distance of penetration shown by the models"? If so, then the bias will simply be the negative of the MAE.

The "average differences" are the Mean Absolute Errors. We have changed the text to clarify the interpretation (lines 275-280). However, it is clear from the Fig. 8a that the model mostly (not always) underestimated the inland penetration in this case.

Sub-section 3.b.2: Consider defining an outline for a reasonable updraft area, then consider only the grid cells there with updrafts, and derive a total flux by multiplying the upward velocity by the area of the grid cells involved. Because maximum updraft is greater for finer resolution, this area-integrated quantity should agree better among the resolutions.

This would be interesting, however, given the scope of this study, this was not the focus of this work.

Line 323: The range (100-1000) should have units of m.

Done.

The labels for panels c and d of Fig. 15 are reversed.

This has been corrected.

The caption for Fig. 16 should start with "The same as Fig. 15…"

This has been corrected.

Line 374: I have trouble with the terms "Mean Bias Error" and "Standard Deviation of Error". I assume that the former is what I am used to being called "mean bias" or just "bias". The latter appears to be a gauge of how much the many individual error values spread from that mean bias. It needs to be precisely defined. You also later refer to MBE of wind direction, which should also be defined with reference to its wrap-around nature (i.e. 359 + 1 = 0). I feel better about RMSE, but you might want to define that also for completeness.

The definitions of MBE, STDE and RMSE are added to the text (lines 401-403, 430). The wind direction metrics have been calculated to take into account its wrap-around nature by calculating the difference using the smallest distance on the circle (lines 412-414).

Lines 390-391: "reducing…up to" is awkward. I suggest "reducing the MBE by as much as 72%". On line 392, I think it is sufficient to insert "by" before "up to". Actually, look for all occurrences of "up to", and I think you should add "by" before nearly all of them.

Done.

Figs. 19 and 20 seem like they could be considered a single figure. The four panels simply correspond to a list of different variables. It can still be split across two pages if necessary.

The two figures have been merged into one figure now.

Lines 420-421: "the decrease in simulated temperature and increase in dew point" is easier to understand and removes "and" and "respectively" while inserting only "in".

Done.

The paper could use an overall editing for grammar and punctuation.

We have edited the paper.

All cases similar to "by maximum 66%" should add two words: "by a maximum of 66%". I don't think you used the word "minimum" in this way.

Done.

Response to Reviewer 2

Major Issues or Fatal Flaws

As I stated above, I was not convinced by the brief discussion of the "mesoscale analysis" used here (section 3a) that a lake breeze was present on 9 August. The presence of a lake breeze must be firmly established, or at least clearly supported, by the text/figures before one can move forward with the rest of the analysis. I did not find this to be the case. Instead, the authors simply say that the mesoscale analysis indicated the presence of a lake breeze (lines 195-197 and lines 208-209). They reference Fig. 2b here, which shows radar reflectivity and surface observations, and state "…gradients along the front were markedly weaker and the front was less well-defined in satellite and radar imagery than was the case for July 15". However, that is more or less the extent of the discussion.

I'm left wondering how exactly it was determined then that this was indeed a lake breeze? In fact, there does not even appear to be a radar fineline present in Fig. 2b over the GTA (at least, it is certainly not obvious from this figure). Surface convergence is weak at best (there are even a few stations north of the magenta line that have weak southeasterly flow). Either way, this figure does not provide nearly enough support for a lake breeze, in my opinion. I understand that the method described in Sills et al. (2011) is used here, but that method does seem to include some amount of user discretion regarding which criteria carry more weight, especially if certain criteria are missing (as was likely the case here).

There are a couple other figures later in the paper (Fig. 10b showing a lidar PPI scan and Fig. 16 showing surface obs at Z2D) that purportedly show evidence for passage of a lake-breeze front. I'll address both of those figures in separate comments below. For now, I'll say that those figures were not very convincing to me and could be improved.

My suggestion is that the authors significantly revise section 3a (and elsewhere in the paper where necessary), explaining in enough detail how they came to determine that this was a lake breeze. What were the determining factors and criteria in each case? This should be done before the model analysis, and for both 15 July and 9 August. Indeed, the 15 July case is much stronger and does appear to feature a lake breeze, but this too did not become clear to me until later in the paper – certainly not during the discussion of the mesoscale analysis.

Since the paper only analyzes two cases, I would think this shouldn't be too cumbersome. However, it must be clear to the reader exactly how this was done, so that it could hypothetically be reproduced, and supported by appropriate arguments and figures so that the reader can follow the authors' train of thought.

I also wonder if there were other cases with non-opposing synoptic flow during the summer of 2015, where the lake breeze is more clearly defined by the observations than on 9 August? If so, perhaps the authors would consider using one of those other cases instead?

We chose two lake-breeze events to represent a strong lake breeze with well-defined gradients on 15 July and a non-classic lake breeze with weak gradients on 9 August. The complete analyses of these two events (with mesonet and lidar) are given in Mariani et al. (2017). The focus of this work on the other hand is to study the performance of the GEM model in predicting these two cases which are good representations of a strong (15 July) and weak (9 August) lake-breeze front. However, we have modified the text to address the issues that the reviewer has mentioned regarding the mesonet analyses. We have also added an Appendix with hourly mesonet analyses for both cases to this paper.

On lines 211-212, it is stated that "The leading edge of the lake breeze in the GEM 0.25 km model output was even less defined, with no discernable updraft zone in the analysis of vertical velocity (Fig. 4)". Later, in lines 237-238, the authors say that "…the GEM 0.25 km failed to generate a clear lake-breeze frontal zone". Again, on lines 246-247, "The GEM 0.25 km model failed to generate the updraft zone of lake-breeze front on August 9…".

Meanwhile, despite these statements indicating that GEM 0.25 km was unable to produce an obvious lake-breeze front, GEM 0.25 km output is still analyzed in section 3b to determine the inland penetration and updraft intensity of the lake-breeze front. For example, "The predicted lake-breeze front with GEM 0.25 km penetrated to maximum 5.6 km at 22:00 UTC…" (lines 255-256). This does not make sense to me.

Then, on lines 249-250, it is stated "Hence, the maximum vertical velocity in thermals at the boundary between two turbulent flows was used to study the impact of the GEM 0.25 km prediction of lake breeze on August 9". So updrafts in thermals are used instead for GEM 0.25 km? This is all very confusing, and not consistent with the method used for 15 July. Perhaps using the maximum updraft isn't the best way to identify the lake-breeze front in the model? Either way, the authors should clarify the approach taken in this section and consider changing how they handle the GEM 0.25 km output to analyze the lake breeze for 9 August, especially if there isn't a lake-breeze front.

We have modified our discussions and figures particularly regarding the GEM 0.25 km results. We agree that in non-classic cases like 9 August 0.25 km case, using the updraft to identify the lake breeze might not be the best way since the updraft zone is not clear. That's why we have modified our method by identifying the boundary between two turbulent and uniform structures as well as wind direction, temperature and dew point changes.

Other Major Comments

(lines 217-218) "The model also predicted a decrease in temperature and an increase in dew point only in areas close to the lakeshore, not along the leading edge of the lake breeze". Is this really a lake breeze? By definition (as the authors correctly state in the Introduction), a lake breeze results from the pressure gradient driven by temperature differences between the water and nearby land. If the lake breeze truly extended as far inland as the authors suggest, then why

do the temperature and dewpoint gradients remain confined to near the lakeshore? Is it also possible that what we are seeing here (Fig. 4) is simply cooler, moist marine air being carried over land by the prevailing synoptic flow?

Also, why not plot Fig. 4 (and Fig. 3) at the time of maximum inland penetration (~1800 UTC instead of 1500 UTC)? Perhaps the temperature and dewpoint gradients are better defined at that time? That also lends support to later figures related to inland penetration.

The gradients for the 9 August case are not as strong as the 15 July case due to lack of an opposing large-scale wind. The decrease (increase) in temperature (dew point) near shore could be the advected marine air, however, we have removed this statement since we have plotted the Fig. 4 at a different time (e.g., 1600 UTC) where the gradients near the front are better defined. We have also plotted Fig. 3 at the time of the maximum inland penetration (2000 UTC).

(lines 221-225) These cross sections could be explained more clearly in the text. It took a few minutes for me to figure out how to interpret them. Maybe say "temporal cross-section" or something of the like to let the reader know that the y-axis is not height, but rather time.

It has been changed to temporal cross-section.

(line 241) What is meant by "enhanced vertical velocity"? Please clarify here or on line 176.

It means "vertical velocity maxima". This has been added to the text (lines 187-188).

(lines 253-254) It says here that the lake-breeze front for GEM 1 km (blue line) reached a maximum distance of 2.8 km at 1900 UTC. What about at 2300 UTC, when GEM 1 km reached ~4 km?

The has been corrected (lines 272-273).

(lines 262-264) This goes back to the discussion regarding GEM 0.25. How was the inland penetration of the lake breeze advection determined if the leading edge (front) of the lake breeze was undetermined?

We have modified our method for this particular case since the updraft zone of the lake-breeze front is not clear. We have used the boundary between the turbulent and uniform flow (i.e. in Fig. 4(b)), change of wind direction to onshore (Fig. 7) and temperature and dew point gradient to determine the inland penetration. We believe this method represent the inland penetration more accurately when the updraft zone associated with lake-breeze front is not clear (lines 263-269).

(lines 276-278) Fig. 10a shows one slice in time at 1424 UTC, so how can it be said to also show that the air flow direction *changed* from offshore to onshore, indicating the passage of the lake-breeze front? Clearly, the blue colors do indicate southerly (onshore) flow, but just one image cannot illustrate the passage of the front. Two images (before/after) would be necessary.

The same can be said for lines 290-292. However, Fig. 10b indicates low-level flow from the east-northeast, more consistent with the prevailing synoptic flow, NOT lake-breeze flow (which was more from the southeast or east-southeast)! This seems to be at odds with the text. Are the authors certain that a lake-breeze front passed through Highway 400 ONroute? Either way, more panels need to be added to Fig. 10 to correctly illustrate a change over time, or it should be removed altogether.

The Fig. 10 is a snapshot illustrating the southerly flow during the lake-breeze passage. The full evolution of the lake-breeze front passage at Hanlan's Point is provided in Figs.4 and 7 from Mariani et al. 2017 (lines 292-294). We have plotted the PPI scan at a different time in Fig. 10b to show the onshore flow more clearly. We have also included two figures (before/after) to the appendix of the authors' response to illustrate the change over time for Highway 400 ONroute. The reference to Mariani et al. (2017) has been added to this section.

(lines 301-303) Fig. 13 is introduced here but the only discussion of the lidar data in this figure is in the figure caption, where it reads "The direction of radial velocity changed from onshore (blue) to offshore (red) at 190 m and 900 m at Hanlan's point and Highway 400 ONroute, respectively". This should be in the text itself. Also, there is still some blue up to ~300 m in Fig. 13a, with the strongest changeover to red occurring closer to 400 m. Furthermore, the direction in which the x-axis is pointing in Fig. 13 is unclear. Is this along the cross-section, toward the south?

The actual changeover from blue to red velocities occurred at 190 m as measured within 100 m from the lidar (lines 323-325). The shape of the LBF on this day was a wedge; hence the changeover altitude sloped upwards further away from the lidar as discussed in Mariani et al. (2017). The text in the paper has been clarified to include "as measured within 100 m from the lidar". The precise changeover altitude may be difficult to discern due to the color value around 0 m/s in the figure as positive (red) velocities occur below 400 m throughout the RHI scan. The direction of the x-axis in Fig. 13 is facing south which is not exactly along the cross-section. The direction of the x-axis has been included in the caption.

(lines 352-357) Is this paragraph referring to Fig. 16? It is unclear to me. If so, the statements made in the text, especially regarding the model comparison, do not match what I see in the figure. First, it is said that the observed temperature decrease and dewpoint increase occur at ~1442 UTC. These changes do not occur until after 1500 UTC (see local temperature max of ~22°C just after 1500 UTC in Fig. 16). Furthermore, it is said that the model predicted a maximum temperature drop and dewpoint increase of 0.2°C and 0.3°C. Maybe so, but these changes are very gradual – starting at ~1300 UTC – and are almost imperceptible to my eyes. There is certainly no abrupt change consistent with the passage of a lake-breeze front. Thus, it seems appropriate to say that the model does not actually suggest the passage of a lake-breeze front.

Furthermore, Figs. 15 and 16 are from a surface station along the shoreline. Why not use an inland station (perhaps the farthest inland station for each case where lake-breeze passage occurred) to bolster the argument that the lake breeze indeed penetrated inland as far as is stated in the text?

The time of the lake-breeze front passage was determined using the time of wind change to onshore(e.g., at 1442 in Fig. 16). In some cases, the passage of the lake-breeze front may or may not be accompanied by a sharp change in temperature and dew point. The change in temperature and dew point can also start a few minutes before/after the wind shift to onshore. The 9 August case was not a classic lake-breeze front. The gradient was not strong due to lack of an opposing large-scale wind. The model may not show the sharp changes in temperature or dew point at every site in this study (model underestimated the drop/rise in temperature/dew point significantly) but it shows the advection of marine air inland and the change of wind direction to onshore. We have plotted Fig. 16 for an inland station which shows the changes due to lake breeze passage more clearly on 9 August.

(Figure 7) It is unclear to me how the vectors are supposed to be interpreted here. Is a vector pointing from bottom right to top left supposed to indicate southeasterly flow, or has it been flipped in some way? This is not stated anywhere in the text or caption. In fact, I'm a bit confused as to what negative horizontal velocity means in this context. Please clarify.

The vector pointing right to left indicates a northerly flow (offshore wind). This has been added to the caption. The limits of the horizontal velocity values have been corrected on the figure colorbar.

10. (Figure 11) Why are the lidar data so shallow here, compared to Fig. 9? In the text, it simply says that the lidar this day had a "limited range of measurements" (line 289). Were there clouds limiting vertical range? Please explain.

The lidar backscatter signal-to-noise ratio was severely reduced at most altitudes > ~200 m for the case of Fig. 11. This is likely attributed to the cleaner, drier air mass measured at this location providing fewer targets (aerosols) for the lidar beam. As a result, the lidar quality control processing algorithm removes data points with a signal to noise ratio below a given threshold, as described in Mariani et al. (2017). This day-to-day variability in lidar vertical range was observed throughout the PanAm Games as it is highly dependent on the local atmospheric conditions at the time. Similarly limited vertical ranges have been observed in Arctic conditions, where a very clean aerosol-free atmosphere persists. To reflect this, the explanation provided in the paper has been expanded to "limited range of measurements due to fewer targets (aerosols) on this particular day at this location" (lines 303-304).

Minor Comments

(throughout) AMS guidelines require dates to follow the format 15 July, 9 August 2015, etc. AMS guidelines also require time to be given in the format hhmm:ss (e.g., 1424 UTC, 1508:31 UTC, etc.). Please adjust throughout the paper.

https://www.ametsoc.org/ams/index.cfm/publications/authors/journal-and-bams-authors/formatting-and-manuscript-components/mathematical-formulas-units-and-time-and-date/

We have changed the format.

(lines 126-127) Where were the other half of the compact stations installed?

We have modified Section 2b as follow:

"During the 2015 Pan/Parapan American Games, 53 automated stations were added to the existing network to increase the spatial density of surface weather observations. The resulting mesoscale network, or 'mesonet', measured 1-minute temperature, dew point, 'black globe' temperature, barometric pressure, wind speed and direction, and precipitation at locations across the GTA. While some stations were located at Games venues, others were set up along or near transects perpendicular to the lakeshore in order to track the inland penetration of the lake-breeze fronts (Joe et al. 2017). Thirteen 'tower' stations measured wind at 10 m AGL and temperature and dew point at 1.5 m (Above Ground Level; AGL), except at the North York location where a shortened tower was installed atop of a low-rise building. The tower stations also measured incoming solar radiation. Twenty all-in-one 'compact' stations measured wind and temperature at 2.5 m AGL, while another 20 made measurements from rooftops of mostly one- and two-story buildings. The compact station data were lightly quality controlled to remove out-of-bound values while the tower station data underwent more thorough quality control. Rooftop locations were chosen only when no suitable ground-level site could be found, most often in highly urbanized areas. No attempt was made to quantify or remove errors introduced by the use of rooftop locations. Table 1 provides information about the particular stations used for this study."

(lines 126-131) Was consideration given to how rooftops would potentially affect temperature measurements? Why were rooftops chosen in these cases? This seems problematic, especially if the compact station data were only lightly QCed.

Please see our reply to the previous comment regarding the first and second part of the comment. Regarding the third comment, we agree that this could introduce extra error but as we stated in the paper rather than comparing the errors at different stations our focus in this paper is to approximately estimate the range of errors during the lake-breeze front passage.

(line 137) I assume "spatial resolution of the radar" refers to the range resolution, since the beamwidth (in meters) increases with range? Please clarify in text.

The King radar has a 0.62 degree beamwidth and the data are sampled at 250m and 0.5°, in range and azimuth resolution, respectively. The radar runs on a 10-minute cycle. This has been added to the text (lines 137-138).

(lines 139-141) Please include a reference or two, perhaps Wilson et al. (1994):

We have included this reference (Wilson et al. 1994).

(line 190 and 194) What is the relevance of reporting the maximum temperature at Toronto International Airport? I suggest removing.

It has been removed.

(lines 174-178) Does GEM natively output data at 10 m and 5 m levels, or are these interpolated from the lowest model vertical levels? If interpolated, please clarify.

GEM natively outputs the data at 5m and 10m. We stated in the text that the model data at prognostic levels were used (line 403-404).

(lined 176) Please explain "enhanced" (also see line 241).

It means vertical velocity maxima (lines 187-188).

(line 231) Panels (a) and (b) in Fig. 6 are not discussed, or at least referred to, at all in the text. Are those panels relevant to the discussion?

We have referred to these panels (line 257).

(line 238) "…possibly due to misrepresentation of convection at thermals and the frontal zone". This statement is confusing, and also speculative. I suggest omitting.

The statement has been removed.

(line 239) "The results also showed that the magnitude of vertical velocity increased for GEM 1 and 0.25 km…". Where does it show that? Which figure(s)/panel(s)?

The comparison of the magnitude of vertical velocity in Fig. 6a (GEM 2.5 km), Fig. 6b (GEM 1 km) and Fig. 6c (GEM 0.25 km) shows that the magnitude increases for GEM 1 and 0.25 km. This is been added to the text (lines 256-258).

(Figure 2) If it is possible to access the radar data, I suggest re-plotting it with a decreased dBZ range (maybe -30 to 10 dBZ) in order to highlight the radar finelines.

Done.

(Figure 2) The station data are very small and difficult to discern. Please enlarge if possible.

Done.

(Figures 3 and 4) I'm not sure if AMS requires this, but the authors may consider plotting longitude as either negative degrees (e.g., -79.6, -79.5, etc.) or as degrees west (e.g., 79.6W, 79.5W, etc.).

Done.

(Figure 3 and others) For color bars that span zero (e.g., Fig. 3a), I strongly suggest using a different color table to more easily delineate between positive and negative values. One similar to that used in Figs. 10 and 13 would be best, with gray or white in the middle (at zero) and warm=position and cool=negative.

We centered the color bars on zero. The green color is set at zero now for vertical velocity plots.

(Figures 5 and 6) Similar to the previous comment, I strongly suggest centering these color bars on zero since it may otherwise be difficult for the reader to differentiate between positive and negative values.

Done.

(Figs 5a, 6a, 9, and 11) For these panels, only a few colors are actually plotted (e.g., ~6 colors for Fig. 5a), resulting in a rather discontinuous appearance of the filled contours. I suggest increasing the number of colors plotted (by decreasing the increment) in order to produce something more visually pleasing, similar to Fig. 5b.

We have increased the number of colors.

(Figs. 15 and 16) To better show the changes in temperature, dewpoint, and wind, I suggest decreasing the y-axis range since there is a lot of unused space in some of the panels (e.g., plotting from 12–24°C in Fig. 15a and 6–14°C in Fig. 15b).

Done.

(Figs. 17 and 18) I suspect that there may be a way to take these two figures and put the data into a table instead. I found them to be a bit confusing in their current form.

We feel the data can be better interpreted through the figure as opposed to a table. The figure also permits visualization of the change in MBE, STDE (etc) values at stations along the PanAm analysis track which would be lost in a table. However, we have modified the figures (merged in one figure; Fig. 17) to more clearly show the results.

(multiple figures) To save some space and condense figures that have multiple panels with the same x-axis, it may be worth it to only label the x-axis on the bottom panel. The panels can then

be moved closer together. This may also result in a more visually pleasing figure anyway. I suggest doing this for Figs. 15 and 16 (and perhaps Figs. 5, 6, 9, and 11).

We have moved the panels closer to each for some figures.

Grammar/Typos

Most of these focus on sections 1 and 2, which I though was well done overall.

(line 39) Perhaps "onshore flow" is a better term to use here than "inflow layer", since the lake breeze might be better thought of as outflow from the lake, not inflow. Also see usage on lines 40-41.

In order to keep it consistent with Sills et al. (2011), we used the term "inflow layer" since we referred to Fig.2 of that paper.

(line 43) Insert "its" before "vicinity".

Done.

(lines 44-45) Remove "the" before "Lake Ontario".

Done.

(line 45) I believe "observational" should instead be "observations".

It is changed to observations.

(line 51) Insert "on" before "over 30% of the days".

Done.

(line 53) Suggest moving the sentence beginning with "In the more recent studies…" to the next paragraph, which also discussed recent studies.

Done.

(line 56) Suggest beginning this sentence with "Other recent studies over southern Lake Ontario have also shown…".

Done.

(line 68) I think it sounds better to remove the "a" before "general agreement".

Done.

(line 75) The word "Lake" at the end of this line shouldn't be capitalized since it doesn't precede "Ontario".

It is changed to "lake".

(line 95) I suggest saying something along the lines of "decreasing the model grid spacing" instead of "increasing the model spatial resolution".

Since the decrease of grid spacing leads to increase of model spatial resolution, we have not changed this.

(lines 99-100) I suggest rewording to something like "Analysis and discussion of the model simulations, including their comparison to ground-based observations, as well as characteristics of lake-breeze fronts are provided in section 3."

Done.

(line 106) Remove the period immediately after "high resolution".

Done.

(line 109) The word "Azimuth" should not be capitalized in this context.

It has been corrected.

(lines 111-112) I suggest rewording this sentence to something like "The second lidar was mounted on the back of a pick-up truck and driven to different locations within the GTA in order to track the lake-breeze front as is transited inland."

Done.

(lines 113-114) I suggest rewording this sentence to something like "The maximum range of the lidar measurements varied from 2 to 5 km depending on weather conditions."

Done.

(line 124) "AGL" is a common abbreviation and AMS doesn't require that you define it (you may still do so if you wish):

https://www.ametsoc.org/ams/index.cfm/publications/authors/journal-and-bams-authors/formatting-and-manuscript-components/list-of-acronyms-and-abbreviations/

The definition is removed.

(line 125) Do you mean "on top of a low-rise building" instead of "at top of a low-rise building"?

This section has been modified.

(line 150) Change "to the 2.5 km domain" to "for the 2.5 km domain".

Done.

(line 189) "…north-easterly (offshore) synoptic flow…" sounds better to me.

We have changed it.

(line 221) The term "Lake-breeze" should not be capitalized.

It has been corrected.

(line 226, 233, and elsewhere) The use of past and present tenses when referring to figures. For example, on line 226: "…Fig. 5 clearly illustrates…" is more appropriate than "…Fig. 5 clearly illustrated…" because we, the readers, are seeing what the figure is showing us now.

This has been corrected.

(line 272) Remove the comma after "(Fig. 9a)".

Done.

(line 417) Remove the "s" in "followings".

Done.

Response to Reviewer 3

General comments:

This manuscript aims to evaluate the ability of Canadian Global Environmental Multiscale Model (GEM) predicting the lake breezes generated by Lake Ontario and assess the impact of model resolutions on the lake-breeze predictions in the Greater Toronto Area (GTA). The authors presented a series of comparisons of different resolutions of GEM simulations (i.e., 2.5km, 1.0 km and 0.25km) with mesoscale analysis, lidar and surface observational data. The results showed that the GEM was successful to predict the lake-breezes for the two events, and increasing model resolution improved the predictions of lake-breeze location, updraft density, and depth. To me, it is a mystery that the GEM was running with a 250m horizontal resolution (see more comments below). Given the large impact of lake breezes on the local weather and air quality near the lakeshores, the study with high resolution numerical model is worthwhile. However, the evaluation and analyses were mainly limited to the selected sites along the cross-section of L1B to A2T. The evaluations with more observational sites will be helpful. The authors should be able to provide statistical evaluations on the GEM simulations (e.g., 2-m air temperature and 10-m winds) with all the available observational data for these two lake-breeze

cases. The manuscript is recommended with major revisions by addressing the following specific comments.

Please see our detailed response in the specific comments section.

Specific comments

The GEM is a global model but was run for the three nested domains with a highest horizontal resolution of 0.25 km for the innermost domain. This is extremely challenging. It is nearly impossible to run a regional model with a horizontal resolution of 250m in terms of stability of numerical solution of partial differential equations that all the numerical weather prediction models rely on. What version of the GEM did you use in this study? What special treatments did you take in order to run a global model at a 250m resolution which is suitable for Large-Eddy Simulations (LESs)? Please highlight the detailed information (e.g., treatment and configurations) which are very important and useful for the readers.

GEM 250 m has been used successfully in previous studies e.g. Lemunsu et al. 2009 (Lemonsu, A., S. Be´ lair, and J. Mailhot, 2009: The new Canadian urban modelling system: Evaluation for two cases from the Joint Urban 2003 Oklahoma City Experiment. Bound.-Layer Meteor., 133, 47–70) and Leroyer et al. 2014 (referenced in the text). GEM 4.6.2 is used in this study. We have included the GEM configuration (including GEM 250 m) in Table 2, however more details on the configuration and treatment for GEM 250 m is given in Belair et al. 2017 (provided in the reference section of the paper)

Accurate simulation of lake surface temperature is important to predict the lake breezes. Did the authors use any lake model for the lake-breeze predictions?

The surface temperature from the NEMO model was used for the lake-breeze prediction. This information has been added to the text (lines 157-159).

As pointed out in the manuscript on Lines 118-119, 53 automated surface weather stations were added to the existing network. How many surface observational sites were there available during the 2015 Pan/Parapan American Games? It will be very helpful if all the observational data are included into the verifications of the GEM predictions during these two lake-breeze cases?

The total number of stations available during the 2015 Pan/Parapan American Games was 70. This paper focuses on the verification of the lake-breeze front passages along the transect that passed through downtown Toronto. Adding all the stations will increase the length of the paper massively. However, we plan to include the observations of other stations in other future papers.

There is nothing wrong with the UTC usage in the manuscript. However, this is very inconvenience for the users who are not familiar with the local time in the GTA. Lake-breeze is a local circulation phenomenon with strong diurnal variation. Local time is much easier for readers to know when the lake breezes started and when they ended. UTC really does not matter. It is strongly recommend using local time rather than UTC for all the analyses and plots.

In order to keep it consistent with the previous work (Mariani et al. 2017) which has been referenced multiple times in this paper, we have used UTC. However, we added a conversion of UTC to local time to the text (lines 204-205).

In several places (e.g., L640, L174-176), the authors mentioned the temperature and dew points at 5 m AGL. To my knowledge, no any measurements were taken and no models generated air temperature output at this height.

The first prognostic level of the GEM model for thermodynamic variables for PanAm runs (e.g. temperature and dew point) was at ~5 m AGL (lines 403-405). The observation altitude of temperature and dew point measurements were different at different stations depending on the station type (Table 1). However, we chose the closest model level to the observations for metric estimation (lines 403-405).

Lines 103-105: Although this study was not focused on the measurements, I believe that some readers are still interested in how the horizontal winds (wind speed and wind direction) and vertical velocity were derived from the lidar measurements.

The radial velocity was estimated by measuring Doppler shifts of backscatters; this was included in the section 2a. The vertical velocity is the radial velocity measured at 90° elevation during staring mode. We have added this information to the text (line 111). The horizontal velocity is estimated using Velocity Azimuth Display (VAD, Browning, K. A. and Wexler, R., The

determination of kinematic properties of a wind field using Doppler radar, J. Appl. Meteor., 7, 103–113, 1968). However, since we did not use lidar-extracted horizontal velocity, we did not include the technique in the paper.

Lines 134-142: How were the winds (horizontal or vertical or both?) derived from the Doppler radar measurements? What are the major differences between Doppler lidar and Doppler radar data since the authors mentioned both in this section?

Similar to lidar, Doppler shifts of backscatters received by radar can be used to calculate radial velocity. The horizontal and vertical velocity can be estimated using the VAD technique. The major difference between lidar and radar data is that the lidar has a higher resolution (3 m) and radar has a larger measurement range. We did not include the radar velocity technique in the paper because we did not use the radar-extracted velocity. However, the radar backscatter was used in mesonet analyses. Some of the important specifications of the lidar and radar are given in Section 2a and 2c, though more details are given in Mariani et al. (2017).

L139-142: What is the "other mesoscale boundaries"? How can we distinguish the lake-breeze fronts from other mesoscale boundaries?

Other mesoscale boundaries include thunderstorm gust fronts, land-breeze fronts, and intense horizontal convective rolls, though lake-breeze fronts and thunderstorm gust fronts were by far the most frequently identified. They are distinguished based on semi-objective criteria described in Sills et al. (2011) but it was ensured that lake-breeze fronts clearly originated from lakes while gust fronts clearly originated from thunderstorms.

L158-159: What are the differences between the thermal and humidity roughness lengths? How they can be used to improve the flux simulations?

The thermal and humidity roughness lengths are the same in the GEM configuration. Unfortunately there were no flux measurements during the PanAm Games, though further studies are planned to assess the impact of roughness length on flux simulations.

L168: Were satellite images from GOES13 used for the analyses in this study?

Yes, the GOES-13 images were used for mesonet analysis. This has been included in the paper (line 171-172).

L169-173: It is better to provide a brief description of the criteria of lake-breeze identification.

We have added a brief description of the criteria to the paper (lines 174-178).

L237-238: Are there any more evidences to support this statement?

We have removed this statement from the text.

Figures 17-20: Why did the authors only present the results at the two sites for the July 15th case?

The focus of this study is to verify the lake-breeze front passage along the transect passing through selected surface stations (e.g., L1B, L1C, etc). The lake-breeze front did not travel inland beyond L1B station on 15 July. Therefore only Z2D (located at shore) and L1B were chosen for these analyses.

Appendix A.

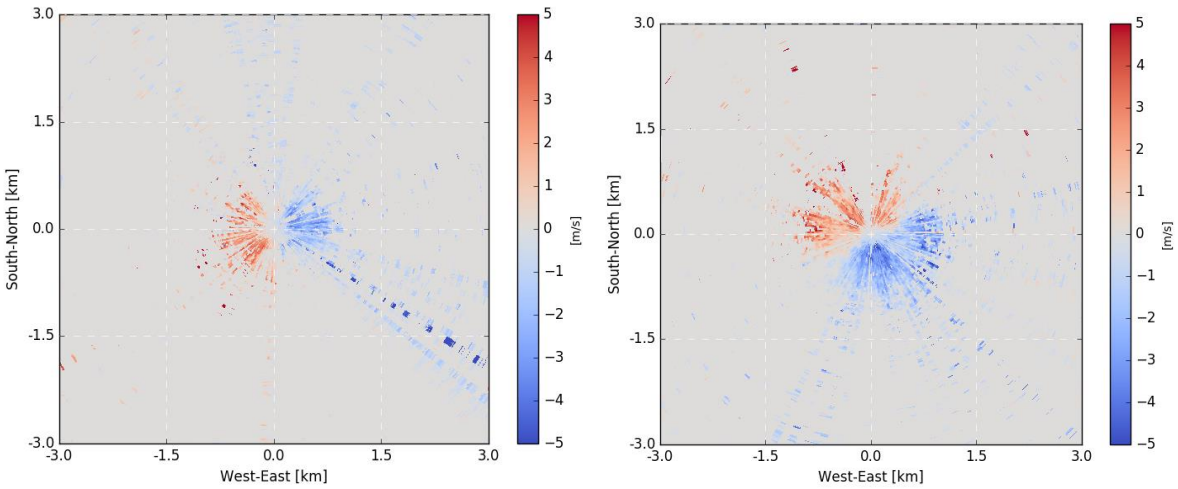

Fig. A1. Lidar measurements of radial velocity in ms^{-1} (PPI scan) at Highway 400 ONroute on 9 August at (a) 1800 UTC and (b) 2037 before and after lake-breeze passage. Negative (blue) velocities represent winds towards the lidar; positive (red) velocities represent winds away from the lidar.

Manuscript (non-LaTeX) Click here to download Manuscript (non-LaTeX) Dehghan et al_final.docx

Evaluation of Modeled Lake Breezes Using an Enhanced Observational Network in Southern Ontario: Case Studies

Armin Dehghan[1], Zen Mariani[1], Sylvie Leroyer[2], David Sills[1], Stéphane Bélair[2] and Paul Joe[1]

[1]Observation-Based Research Section, Environment and Climate Change Canada, Toronto, Canada
[2]Environmental Numerical Prediction Research, Environment and Climate Change Canada, Dorval, Canada

Abstract:

Canadian Global Environmental Multiscale (GEM) numerical model output was compared to the meteorological data from an enhanced observational network in order to investigate the model's ability to predict Lake Ontario lake breezes and their characteristics for two cases in the Greater Toronto Area (GTA) – one where the large-scale wind opposed the lake breeze and one where it was in the same direction as the lake breeze. The enhanced observational network of surface meteorological stations, a C-band radar and two Doppler wind lidars were deployed among other sensors during the 2015 Pan/Parapan American Games in Toronto. The GEM model was run for three nested domains with grid spacings of 2.5, 1 and 0.25 km. Comparisons between the model predictions and ground-based observations showed that the model successfully predicted lake breezes for the two events. The results indicated that using GEM 1 and 0.25 km increased the forecast accuracy of the lake-breeze location, updraft intensity and depth. The accuracy of the modeled lake breeze timing was approximately ±90 minutes. The model under-predicted the surface cooling caused by the lake breeze. The GEM 0.25 km model significantly improved the temperature forecast accuracy during the lake-breeze circulations, reducing the bias by up to 72%, but it mainly under-predicted the moisture and over-predicted the surface wind speed. Root Mean Square Errors of wind direction forecasts were generally high due to large biases and high variability of errors.

Corresponding Author: Armin Dehghan, armin.dehghan@canada.ca

1. Introduction

The 2015 Pan American and Parapan American Games from 10 July to 15 August provided Environment and Climate Change Canada (ECCC) with a unique opportunity to undertake an extensive observation campaign in the Greater Toronto Area (GTA) including a mesoscale network specifically designed to detect and track lake breezes, and in particular the lake-breeze front (Joe et al. 2017). Additionally, two Doppler lidars (hereafter referred to as lidars) provided real-time observations of winds. The Canadian Global Environmental Multiscale (GEM) numerical model was run at the horizontal grid spacings of 2.5, 1 and 0.25 km to study its ability to predict lake breezes and urban meteorology.

Lake breezes develop due to the temperature contrast between air over cool lake water and air over the warm land surface (Atkinson 1981; Pielke 1984). The thermal contrast produces a pressure difference between the lake and land that forces cooler air inland off the lake. Fig. 2 of Sills et al. (2011) shows an idealized lake breeze circulation. The lake-breeze front develops at the leading edge of the inflow layer. The surface convergence and updraft at the lake-breeze front can generate a narrow band of convective clouds (Lyons 1972). The depth of inflow layer typically ranges from 100 to 1000 m (Lyons 1972; Keen and Lyons 1978; Curry et al. 2016; Mariani et al. 2017), however, the return flow above the inflow layer can be twice as deep (Lyons 1972).

The GTA is often affected by lake breezes due to its proximity to Lake Ontario. Estoque et al. (1976) investigated the structure and diurnal variations of lake breezes over the southern part of Lake Ontario using both observations and numerical simulations. The passage of the lake-breeze front was marked by a sharp shift in wind direction, decrease in temperature, and increase in

relative humidity. Estoque et al. (1976) also showed that the lake-breeze front depth can reach 250 m, and the lake breeze can penetrate as far as 30 km inland. Comer and McKendry (1993) extended the work of Estoque et al. (1976) by investigating a wider range of data. They used the lake-breeze index developed by Biggs and Graves (1962) to identify lake breezes. They found that lake breezes developed on over 30% of the days during summer over Lake Ontario and could penetrate as far as 45 km inland. They also suggested that the wind field over Lake Ontario can be influenced significantly by nearby lakes.

In the more recent studies of lake breezes in the GTA, it was found that GTA lake breezes occurred on more than 70% of warm season days (Wentworth et al. 2015; Mariani et al. 2017). Other studies of lake breezes in southern Ontario have shown that lake breezes can penetrate as far inland as 215 km (Sills et al. 2011), initiate thunderstorms (Sills et al. 2002; King et al. 2003) and affect air quality (Hastie et al. 1999; Hayden et al. 2011; Wentworth et al. 2015). Lake breezes have a large influence on the meteorology and climate of coastal cities particularly in spring and summer, and it is therefore important to forecast lake breezes accurately.

Previous modeling studies of Lake Ontario lake breezes are limited to numerical models with grid spacings of 20 and 10 km (Estoque and Gross 1981; Comer and McKendry 1993). Estoques and Gross (1981) used a primitive equation model (e.g., momentum, thermodynamic continuity equations) with variable grid spacings of 20 km (along x axis of domain) and 10 km (along y axis of domain) and five vertical levels. They compared the simulated lake breeze with observations for one day. Their results showed that the effect of prevailing flows and orography were important in simulating the characteristics of the lake breeze. The comparison of the simulated and observed lake-breeze front showed general agreement. It was suggested that the detailed differences (e.g., lake-breeze location and convergence zone) were due to deficiencies of

71 the model equations, unrealistic initial conditions and a flat terrain. Comer and McKendry (1993)
72 simulated Lake Ontario breezes using the Colorado State University (CSU) mesoscale model
73 with grid spacings of 40 km for the main domain and 10 km for the nested domain. Simulations
74 with four different gradient wind directions showed generally good agreement with observations.
75 However, the model underestimated the inland penetration of lake breezes. They also showed
76 that the Lake Ontario lake breeze was strongly influenced by the size and shape of the lake as
77 well as the large-scale wind direction.

78 Sills et al. (2011) identified the lake-breeze fronts using GEM 2.5 km simulations over the Great
79 Lakes. The model showed some ability to predict lake breezes successfully. However, the timing
80 and locations of the lake-breeze fronts did not always match the observations in detailed case
81 studies over the Lake Erie, Lake St. Clair and Lake Huron. The Lake Ontario and Toronto region
82 were not included in their study. Leroyer et al. (2014) studied the sea-breeze events around the
83 urban coastal area of Vancouver using GEM with grid spacings of 2.5, 1 and 0.25 km. Results
84 showed that although GEM 2.5 and 1 km provided accurate near-surface meteorological
85 variables (e.g., temperature, wind speed and wind direction), the physical processes involved
86 with sea-breeze fronts (e.g., sea-breeze inland penetration, interaction with large-scale flow)
87 were handled better with GEM 0.25 km. Kehler et al. (2016) examined 56 cases of lake breezes
88 over Lake Winnipeg and Lake Manitoba. They showed that GEM 2.5 km correctly simulated
89 78% and 68% of the Lake Winnipeg and Lake Manitoba lake breeze occurrences, respectively.

90 During the Pan/Parapan American Games, in addition to ground-based observations, the
91 experimental high-resolution GEM 1 and 0.25 km were run semi-operationally for the first time
92 for the GTA and Lake Ontario to support the weather forecast program and to evaluate the high-
93 resolution GEM forecasts. Mariani et al. (2017) demonstrated that synoptic winds had an

94 important impact on the characteristics of the lake-breeze fronts in the GTA during the Games.
95 Thus, the main objective of this paper is to test the ability of the GEM model to predict Lake
96 Ontario lake breezes under two different synoptic wind regimes, and to determine if increasing
97 the model spatial resolution improves the forecast of lake-breeze characteristics. The ground-
98 based observational network is used to verify the accuracy of predicted temperature, dew point
99 temperature, wind speed and wind direction. The data, model design and lake-breeze
100 identification methods are presented in Section 2. Analysis and discussion of the model
101 forecasts, including their comparison to ground-based observations and characteristics of lake-
102 breeze fronts are provided in Section 3. The conclusions are given in Section 4.

103 ## 2. Data and methodology

104 a. Doppler lidar data

105 ECCC's HALO Doppler lidar provide high-resolution (3 m) radial velocity measurements by
106 measuring the Doppler shift of the backscattered pulse from aerosols. This allows remote
107 observation of the horizontal and vertical structure of lake-breeze circulations at high resolution
108 (Darby et al. 2002; Tsunematsu et al. 2009; Mariani et al. 2017). During the 2015 Pan/Parapan
109 American Games, two scanning lidars operated in constant elevation (Plan Position Indicator;
110 PPI), constant azimuth (Range Height Indicator; RHI), and vertically staring modes. The vertical
111 velocity was estimated by measuring radial velocity at 90° elevation (staring mode). One of the
112 lidars was deployed at Hanlan's Point (43° 36' 44" N, 79° 23' 19" W) on Toronto Island and
113 operated continuously. The second lidar was mounted on the back of a pick-up truck and driven
114 to different locations within the GTA in order to track the lake-breeze front as is transited inland.
115 The maximum range of the lidar measurements varied from 2 to 5 km depending on weather

conditions. The lidar measurements conducted at Hanlan's Point and Highway 400 ONroute (43° 53' 38" N, 79° 33' 26" W) will be used in this study.

b. Mesonet data

During the 2015 Pan/Parapan American Games, 53 automated stations were added to the existing network to increase the spatial density of surface weather observations. The resulting mesoscale network, or 'mesonet', measured 1-minute temperature, dew point, 'black globe' temperature, barometric pressure, wind speed and direction, and precipitation at locations across the GTA. While some stations were located at Games venues, others were set up along or near transects perpendicular to the lakeshore in order to track the inland penetration of the lake-breeze fronts (Joe et al. 2017). Thirteen 'tower' stations measured wind at 10 m AGL and temperature and dew point at 1.5 m AGL, except at the North York location where a shortened tower was installed atop of a low-rise building. The tower stations also measured incoming solar radiation. Twenty all-in-one 'compact' stations measured wind and temperature at 2.5 m AGL, while another 20 made measurements from rooftops of mostly one- and two-story buildings. The compact station data were lightly quality controlled to remove out-of-bound values while the tower station data underwent more thorough quality control. Rooftop locations were chosen only when no suitable ground-level site could be found, most often in highly urbanized areas. No attempt was made to quantify or remove errors introduced by the use of rooftop locations. Table 1 provides information about the particular stations used for this study.

c. Doppler radar data

The C-band Doppler radar used in this study was located north of Toronto in King City (43° 57' 50" N, 79° 34' 26" W). The radar operated at 5625 MHz frequency with a beamwidth of 0.62°.

Data are sampled at 250 m and 0.5°, in range and azimuth resolution, respectively. The radar runs on a 10-minute cycle. (Hudak et al. 2006; Boodoo et al. 2010). These measurements cover the GTA and Lake Ontario. Radar "fine lines" are often observed and are due to the presence of insects along the updrafts of lake-breeze fronts and other mesoscale boundaries (Wilson et al. 1994). The radar fine lines can be used along with other observations to track lake-breeze fronts (Sills et al. 2011).

d. GEM model data

The GEM atmospheric model was originally developed in the 1990s at ECCC (GEM; Côté et al. 1998; Zadra et al. 2008). It is based on a fully implicit temporal solution on staggered vertical and horizontal grids (Girard et al. 2014). A full suite of physical processes is represented in the GEM model (Bélair et al., 2003a, b). The model data used in this study were produced following the configuration established for Pan/Parapan American Games project. Most of the features were similar to those in Leroyer et al. (2014) and Bélair et al. (2017), and included three nested domains with grid spacings of 2.5, 1 and 0.25 km (see Fig. 1) and 57 vertical levels. The output of the Regional Deterministic Prediction System (RDPS; Fillion et al. 2010) with a grid spacing of 10 km provided initial and hourly boundary conditions for the 2.5 km domain. A summary of physics schemes, time steps, horizontal grid spacing and vertical levels is provided in Table 2. In order to simulate lake-breeze flows, accurate differential heating between the lake and the land is required. Therefore, in addition to previous configurations, surface temperatures for the Great Lakes were prescribed using 2-km hourly output from a coupled ocean-atmosphere forecasting system (Dupont et al. 2012) using the Nucleus of European Model of the Ocean (NEMO) for the daily runs. For the remaining water bodies over the model domains, direct output from the 10-km RDPS and analyses based on buoys and satellite data (Brasnett 2008) were used. Turbulent

fluxes were calculated for different surface types (Bélair et al. 2003a; Leroyer et al. 2010), and over the water, they were estimated using the aerodynamic roughness length of Charnock (1955). Furthermore, the thermal and humidity roughness length of Deacu et al. (2010) was used since they found an improvement of the fluxes simulations over Lake Ontario. The model also used the advanced double-moment microphysics scheme of Milbrandt and Yau (2005). The land surface model of the Interaction between Surface, Biosphere and Atmosphere (ISBA, Noilhan and Planton 1989; Bélair et al. 2003a, b) and Town Energy Balance (TEB; Masson 2000) represented land surface physical processes over natural and urban land surfaces, respectively.

e. Lake-breeze identification methods

The analysis approach described in Sills et al. (2011) used mesonet data including temperature, dew point, wind speed and wind direction measurements, satellite images from GOES-13, and the C-band radar reflectivity to identify the lake-breeze front. The criteria for the identification of lake-breeze fronts are given in Table 1 of Sills et al. (2011). Briefly, they include:

- A cumulus cloud line and/or radar fine line quasi-parallel to shore and either quasi-stationary or moving inland,
- An elongated area of converging near-surface winds quasi-parallel to shore and either quasi-stationary or moving inland, and
- A rapid shift in wind direction to onshore as the lake breeze moves inland.

It is noted that the signal associated with the lake-breeze front may be undetectable or very subtle in each of satellite, radar and surface data, and the use of all three observational platforms improves the likelihood of identification. Additionally, the lake-breeze front may be

accompanied by a rapid change in wind speed and a sharp decrease (increase) in temperature (dew point). When all data were available, the mesoscale analysis error associated with the lake-breeze front position was estimated to be ± 1km.

The GEM forecasts of a wind direction shift (at ~10 m AGL), decrease in temperature (at ~5 m AGL) and increase in dew point (at ~5 m AGL) were used to identify lake breezes at 15 minute intervals. Additionally, predicted vertical velocities were analyzed since when enhanced (i.e., when the vertical velocity maxima occurs) they could also be an indicator of a lake-breeze front (Harris and Kotamarthi 2005; Sills et al. 2011). The vertical velocities at ~120 m AGL were used in order to minimize near-surface effects.

3. Results and discussions

The mesoscale and lidar analyses over the GTA (Mariani et al. 2017; see also the appendix A for mesoscale analyses) indicated that the lake-breeze front on 15 July, 2015 was slow-moving with limited maximum inland penetration of 6 km under a northerly/north-north-easterly synoptic wind (opposing flow). The front remained inland from the shore for ~10 hours before it retreated somewhat then dissipated. In contrast, the lake-breeze front on 9 August, 2015 was fast-moving, traveling more than 60 km inland within ~5 hours under easterly/east-north-easterly synoptic winds (non-opposing flow). The primary purpose of this section is to determine whether the high-resolution GEM model predicted the characteristics and impact of the lake breezes under the two different synoptic flows.

a. Lake-breeze events

High surface pressure dominated the GTA with northerly/north-north-easterly (offshore) synoptic flow on 15 July, 2015. The mesoscale analysis showed that the surface wind shifted to

south/south-westerly as the lake-breeze front passed the lakeshore at 1508 UTC (Toronto local time+5). The lake-breeze front traveled 6 km inland before it began to retreat lakeward at 2000 UTC. On 9 August, the easterly/east-north-easterly synoptic flow was dominant throughout the day. Mesoscale analyses (Fig. A2) showed that the lake-breeze front developed at the eastern part of the lakeshore at 1400 UTC and extended to the western part of the GTA by 1500 UTC. The lake-breeze front reached its maximum distance of 60 km in the GTA at 2300 UTC.

Figs. 2-4 show examples of mesoscale and GEM model output analyses used for identification of lake-breeze fronts on 15 July and 9 August. Fig. 2a illustrates that the observed wind was north-easterly ahead of the lake-breeze front at 2000 UTC on 15 July. This was captured by GEM 0.25 km, which predicted north-easterly/north-westerly winds in Fig. 3b. The predicted vertical velocity plot for 15 July (Fig. 3a) shows that the model generated a narrow updraft zone parallel to the lakeshore coinciding with a wind shift to onshore, decrease in wind speed (Fig. 3b), a decrease in temperature (Fig. 3c) and an increase in dew point (Fig. 3d). The position of the updraft zone was similar to the position of the observed lake-breeze front (magenta line in Fig. 3).

The mesoscale analyses identified the lake-breeze front on 9 August at 1600 UTC (Fig. 2b). However, due to the onshore synoptic-scale flow, gradients along the front were markedly weaker and the front was less well-defined in satellite and radar imagery than was the case for 15 July. The leading edge of the lake breeze in the GEM 0.25 km model output was not clearly defined in the analysis of vertical velocity (Fig. 4a). However, similar to the 15 July case, the model produced more turbulent boundary-layer flow deeper inland (depicted in the upper portion of the Figs 4a-b) and more uniform boundary-layer flow close to the Lake Ontario. This suggests that the model predicted the suppressing effect of the relatively cool marine air on thermal

developments due air advection from the lake. The model also predicted a decrease in temperature and an increase in dew point close to the leading edge of the observed lake-breeze front but with weaker gradients compared to the 15 July case.

b. Lake-breeze front characteristics

1) Inland penetration

The inland penetration distance of the lake-breeze front was examined using the interpolation of vertical velocity for 100 points along the shore-A2T cross-section (red line in Figs. 3a-4a). Figs. 5-6 show the temporal cross-section of vertical velocities for 15 July and 9 August, respectively. Since the distance between the shore and A2T along the cross-section is 28 km, the values are given to the nearest 0.28 km due to the density of points used along the transect but it is realized that the uncertainty is larger than that, depending on the grid size used. The intersections of the observed lake-breeze fronts (mesoscale analyses) with the cross-section were also determined and marked in Figs. 5-6.

The predicted vertical velocity maxima in Fig. 5 clearly illustrates that the updraft zone moved inland slowly on 15 July and retreated to the lakeshore in agreement with mesoscale analyses. However, the predicted updraft zone of maximum vertical velocity with GEM 0.25 km was not continuous (Fig. 5c) since the model tended to resolve smaller structures of updrafts and downdrafts. This was more evident in the 9 August case since the high-resolution model produced more thermals in this case.

On 9 August, GEM 0.25 km produced two different regimes of vertical motions in Fig. 6c; one with smaller updraft structures ahead of the observed lake-breeze front and another with elongated structures behind the observed lake-breeze front. The boundary between the two flow

249 regimes moved inland in the proximity of the observed lake-breeze front. Fig.7 also illustrates
250 the horizontal wind shift of north-easterly (offshore) to south-easterly (onshore) flow, suggesting
251 the lake breeze passage even though the updraft zone of lake-breeze front was not clear (Fig. 6c).
252 It appears that the GEM 0.25 km model produced a weak convergence zone along the leading
253 edge of the lake breeze (due to lack of opposing wind) in this case and at the same time resolved
254 the larger eddies. This makes it more challenging to locate the lake-breeze front using enhanced
255 vertical velocity.

256 The results also showed that the magnitude of vertical velocity increased for GEM 1 and 0.25 km
257 (Figs. 5b-c, 6b-c) compared to GEM 2.5 km (Figs. 5a, 6a), while the width of the updraft zone
258 decreased. The width of the updraft zone was defined as the width of the enhanced vertical
259 velocity zone. As a result, GEM 0.25 km produced an updraft zone with a width of less than 2
260 km on 15 July. Lake-breeze fronts are generally less than 2 km in width (Lyons 1972; Curry et
261 al. 2016). Hence, GEM 0.25 km represented the lake-breeze width better in this case.

262 The distance traveled by the predicted lake breeze (Fig. 8) was determined by locating the
263 maximum vertical velocity in the updraft zone. Since the updraft zone of the lake-breeze front is
264 not clear in the vertical velocity plots generated by GEM 0.25 km on 9 August, the boundary
265 between the uniform and turbulent flows (Fig. 4b), wind direction changes to onshore (Fig. 7)
266 and gradients of temperature and dew point (Fig. 4c-d) were visually located for estimation of
267 the lake breeze inland penetration. This method may not be as accurate as locating the enhanced
268 vertical velocity (when it is clearly defined) but it can be used to approximately locate the lake
269 breeze penetration in this case. The results were compared to the inland penetration of the lake-
270 breeze fronts identified by mesoscale analysis. While the observed lake-breeze front reached its
271 maximum distance from the lakeshore (~6 km) at 2000 UTC on 15 July, the predicted lake-

breeze fronts with GEM 2.5 and 1 km reached their maximum distance of 2.2 and 3.9 km at 1700 and 2300 UTC, respectively. The predicted lake-breeze front with GEM 0.25 km penetrated to maximum 5.6 km at 2200 UTC before it retreated to the lakeshore. The model mostly underestimated the inland penetration in this case. The Mean Absolute Error (MAE) of the predicted inland penetrations from 1700 to 2300 UTC, were 2.3, 2.4 and 0.9 km for GEM 2.5, 1 and 0.25 km, respectively. On 9 August, the model initially underestimated the inland penetrations but the predicted lake breeze traveled deeper inland than the observed lake breeze after one hour with GEM 2.5 and 1 km and after half an hour with GEM 0.25 km (Fig. 8b). The MAE of the predicted lake breeze penetrations from 1500 to 1700 UTC was 2.5, 1.1 and 2.3 km with GEM 2.5, 1 and 0.25 km, respectively. Overall, the location of the lake-breeze front was predicted more accurately with GEM 0.25 km on 15 July and with GEM 1 km on 9 August.

2) Updraft intensity

The intensity of the lake-breeze updraft was determined by measuring the maximum vertical velocity. Fig. 9 shows the vertical profiles of vertical velocities at the Hanlan's Point site from 1400 UTC on 15 July until 0000 UTC on 16 July. The positive (updraft) and negative (downdraft) vertical velocities measured by lidar (Fig. 9a) were associated with convective mixing in the atmospheric boundary layer. Lidar measurements exhibited an increase of updraft intensity at 1423-1431 UTC extending from surface to about 600 m. The maximum vertical velocity of 2.3 ms^{-1} was measured at 1427 UTC at the altitude of 310 m AGL. Furthermore, the lidar PPI scan of Lake Ontario at 1424 UTC in Fig. 10a shows that the air flow direction changed from offshore to onshore, indicating the passage of lake-breeze front (the full evolution of the lake-breeze front passage at Hanlan's Point is provided in Figs. 4 and 7 from Mariani et al. 2017). The GEM 2.5, 1 and 0.25 km predicted that the maximum vertical velocity occurred later

295 at 1645, 1600 and 1600 UTC, respectively (Figs. 9b-d). Similar to Fig. 5, by increasing the
296 model resolution, the updraft zone narrowed and the vertical velocities increased in Figs. 9b-d.
297 The maximum vertical velocities of 0.2 and 0.5 ms^{-1} were predicted with GEM 2.5 and 1 km,
298 respectively. These values are significantly smaller than the lidar observation of the lake-breeze
299 updraft. The GEM 0.25 km predicted higher maximum vertical velocity of 1.9 ms^{-1} at 365 m
300 AGL. This suggests that the increase of model resolution improved the representation of the
301 updraft intensity, though it did not improve the accuracy of the updraft timing in this case.

302 The profiles of vertical velocity for the 9 August case at the Highway 400 ONroute site are
303 presented in Figs. 11 and 12. The mobile lidar operated from 1800 to 2100 UTC; its range was
304 limited due to fewer targets (aerosols) on this particular day at this location. The maximum
305 vertical velocity of 3.3 ms^{-1} was measured at 1819 UTC at an altitude of 230 m AGL (Fig. 11a
306 and 12). Additionally, the PPI scan in Fig. 10b illustrates that the wind shifted to onshore flow at
307 1827 UTC, indicating the passage of lake-breeze front. The predicted vertical velocities in Fig.
308 11b for the period of 1400 to 2100 UTC shows that maximum vertical velocity of 0.17 ms^{-1}
309 occurred at 760 m AGL at 1815 UTC. Figs. 11c-d show that GEM 1 and 0.25 km resolved
310 smaller structures producing more updrafts compared to GEM 2.5 km. Near to the time of the
311 observed lake-breeze front passage, GEM 1 km predicted the maximum vertical velocity of 0.75
312 ms^{-1} at 1800 UTC at 760 AGL (Fig. 11c) and GEM 0.25 km predicted the maximum of 2.6 ms^{-1}
313 at 1715 UTC at 605 m AGL (Fig. 11d). These updraft zones are vertically more extended than
314 the ones predicted earlier (at 1515 and 1615 UTC) which could suggest that they are more likely
315 associated with the lake-breeze front rather than convective rolls. Results also show that the
316 order of magnitude of lidar maximum vertical velocity for the available measurements (Fig. 12)
317 was more comparable to the GEM 0.25 km prediction of vertical velocity (Fig. 11d). The timing

of the maximum vertical velocity did not change significantly for different resolutions of the model.

3) Depth

The RHI scans taken at Hanlan's Point and Highway 400 ONroute (Fig. 13) were used to find lake-breeze depths by determining the altitude at which the direction of radial velocity changed from onshore to offshore. The strongest changeover of the radial velocity direction from onshore (blue) to offshore (red) occurred at 190 m and 900 m as measured within 100 m from the lidar at Hanlan's point and Highway 400 ONroute, respectively. Similarly the modeled lake-breeze depth was estimated by locating the altitude at which the horizontal velocity changed to an offshore wind. Fig. 14 shows the observed and predicted lake-breeze depths for 15 July and 9 August. The results in Fig. 14a indicates that the depth increased after the lake-breeze front passage at 1424 UTC on 15 July, and decreased after the lake breeze dissipated at Hanlan's Point. The comparisons between GEM output and lidar-measured depth showed that the model did not generate any lake-breeze depth until 1615 UTC due to the late lake-breeze front model timing. The model underestimated the lake-breeze depth on average by 83 and 37 m with GEM 2.5 and 1 km, respectively, and overestimated by 27 m with GEM 0.25 km from 1630 to 2315 UTC.

On 9 August, GEM 2.5, 1 and 0.25 km overestimated the depth by 255, 133 and 143 m, respectively from 1815 to 2045 UTC (Fig. 14b). While the GEM predictions of the lake-breeze depth were generally larger than observations, GEM 0.25 km predicted closer values to the observations within 45 minutes from the time the observed lake-breeze front passed over the lidar site at ~1815 UTC. The GEM 0.25 km initially underestimated the depth by 28 m from

1830 to 1900 UTC, but the error increased after 1900 UTC. One should note that both measured and predicted lake-breeze depths on this day were larger than depths on 15 July likely due to greater low-level instability in the atmosphere which could encourage an extension of the lake breeze vertical structure (Atkinson 1981).

Overall, GEM 1 and GEM 0.25 km performed better in predicting the lake-breeze depth for the two events. Both the measured and predicted lake-breeze depths were within the ranges (100-1000 m) of previous studies of lake-breeze depth (Lyons 1972; Curry et al. 2016).

c. Lake-breeze front impact

Time series of 1-minute observations at selected surface stations (Table 2) are used to examine the accuracy of the predicted temperature drop, dew point rise, horizontal wind speed decrease and timing of wind shift to onshore upon arrival of the lake-breeze front. The wind shift timing using 1-minute data was selected to match the timing of the mesoscale analyses. The decrease in temperature and increase in dew point were estimated from 15 minutes before the wind shift until 45 minutes after, since the change in temperature and dew point can begin slightly earlier than the wind shift. A similar method was used to analyze the model output. The results are presented in Table 3. The decrease in wind speed due to the lake-breeze front is not included in the table since it was only observed at Z2D and L1B on 15 July, and at L1F on 9 August. Figs. 15-16 show the time series of temperature, dew point, wind direction and wind speed at Z2D station for 15 July and at L1F for 9 August.

On 15 July, the temperature dropped 1.3°C and the dew point rose 1.6°C at 1508 UTC at Z2D. The offshore wind (1°-90° and 270°-360°) also shifted to onshore (90°-270°) and the wind speed decreased by ~1 ms^{-1} indicating that lake-breeze arrived at the station. Comparisons of the GEM

output with observations showed that the model failed to capture the sharpness of the wind direction changes possibly due to diffusive processes in the model. The model also predicted a smaller drop in temperature at 1615-1630 UTC. A maximum temperature decrease of 0.9°C and maximum dew point increase of 0.7°C were predicted by the model. The ground-based observations also showed that the lake-breeze front reached the L1B site at 1845 UTC and remained quasi-stationary until 2030 UTC causing a temperature drop of 2.3°C, dew point rise of 3°C and wind speed decrease of ~1 ms^{-1}. The lake-breeze front retreated slowly arriving at the lakeshore at 0000 UTC on 16 July. The model predicted a similar pattern though it could not propagate the front to the L1B station (see Fig. 5). As a result, the model did not predict any wind shift or temperature decrease (except with GEM 0.25 km), but predicted the increase in dew point.

The observations on 9 August showed a decrease of 1.4°C in temperature, an increase of 1.1°C in dew point and a change of wind direction from offshore to onshore at ~1442 UTC (Table 3); no sharp changes in wind speed was observed at Z2D. The model predicted the maximum temperature drop and dew point increase of 0.2°C and 0.3°C, respectively, for this station. The impact of the lake-breeze front was more significant at some of the stations located deep inland. For example, ~23 km from the lakeshore at L1F station (Fig. 16), the offshore wind shifted to onshore at ~1648 UTC, indicating lake-breeze front passage at this location. The lake-breeze front passage dropped the temperature by 1.5°C and increased the dew point by 2.5°C. However, the model predicted a maximum decrease of 0.3°C in temperature and maximum increase of 1°C in dew point at this station. The wind speed observations showed a decrease of ~1 ms^{-1} while GEM 1 and 0.25 km predicted a decrease of 2 ms^{-1}. The GEM 2.5 km model did not produce any decrease in wind speed during the lake breeze passage.

The model consistently underestimated the temperature drop associated with the lake-breeze front for all examined cases in this study. The errors of the predicted temperature drops ranged 0.4-2.5°C and were reduced by up to 30% by increasing the model resolution except at Z2D. The model also underestimated the increase in dew point by up to 2.1°C. The predicted lake-breeze front (wind shift) timing was late by a maximum 82 minutes for stations close to lakeshore and early by a maximum 98 minutes for stations located deep inland. The increase of model resolution improved the prediction accuracy of timing at all the stations except at L1B.

d. Near-surface meteorological variables

The predicted temperature, dew point, wind direction and horizontal wind speed were compared to ground-based observations to evaluate the performance of the model from the time the lake-breeze fronts arrived at the surface station until the time the lake-breeze circulations ended. Following the approach in Sills et al. (2011), the end time was defined as the last hour that the lake breeze could be seen on the lakeshore. Therefore, the time at which the wind shifted to offshore was considered to be the end time of the lake-breeze circulation. For example, on 15 July, the model was evaluated at Z2D from the arrival time of lake-breeze front at 1508 UTC until the end of the circulation at 0100 UTC on 16 July.

Fig. 17 shows the Mean Bias Error (MBE) and Standard Deviation of Error (STDE) estimated at 15 minutes intervals on 15 July and 9 August. The MBE and STDE represent the mean bias and the deviation of errors from the mean bias, respectively. The model data at the first prognostic level (~10 m for wind and ~5 m for temperature and dew point) were used for calculating the metrics since this was the nearest level to the altitudes of observations (2.5-10.3 m AGL). In addition, the lake-breeze circulation timing during which the metrics were calculated varied

407 depending on the lake-breeze front arrival time. Therefore, the errors at surface stations cannot
408 be compared directly. Nevertheless, the focus of this section is to obtain a range of errors during
409 the lake-breeze events rather than comparing the results of different surface stations.

410 The results indicate that the GEM 2.5 km model underestimated temperature by 1.4-3.6°C in
411 both case studies at all the selected stations. It also overestimated the dew point by 0.6-3°C
412 except at Z2D (both cases) and A2T stations. The wind direction errors were determined by
413 estimating the difference using the smallest distance on the circle to account for its wrap-up
414 nature (i.e. 359+1=0). The wind direction MBEs were high ranging from 9° to 93°. The wind
415 direction errors were particularly large at L1B on 15 July since no lake-breeze front was
416 predicted for the L1B station. The predicted wind direction remained offshore during most of the
417 day at this location leading to large errors during the lake-breeze circulation. The wind speed was
418 overestimated on 15 July and underestimated on 9 August with GEM 2.5 km. The wind speed
419 MBE ranged from 0.1 to 2.2 ms^{-1} with GEM 2.5 km. The increase of model resolution (grid
420 spacings of 1 and 0.25 km) improved the accuracy of temperature prediction, reducing the MBE
421 by as much as 72%. GEM 1 and 0.25 km mostly underestimated the dew point and
422 overestimated the wind speed. The MBEs of dew point and wind speed were reduced at some
423 stations (e.g., L1E) by up to 86% with GEM 1 and 0.25 km. The increase of model resolution did
424 not reduce the wind direction MBE significantly, except at L1B on 15 July. The results also
425 showed that the wind direction errors had the highest variability (STDE) compared to
426 temperature, dew point and wind speed. This was expected due to natural variability of wind
427 direction and inability of numerical models to accurately capture these variabilities and the
428 timing of wind shifts (Hanna 1994; Harris and Kotamarthi 2005).

The forecast accuracy was determined by estimating Root Mean Square Errors (RMSE). The RMSE represents the deviation of forecasts from observations. The RMSE values of temperature, dew point, wind direction and wind speed ranged over 0.6-3.6˚C, 0.7-3.1˚C, 19˚-126˚ and 0.6-2.4 ms^{-1}, respectively. In order to find the confidence interval of RMSE values, the bootstrap method (DiCiccio and Efron 1996) was used. The method is based on resampling with replacement from the given sample. For this work, the errors (forecast-observation) were resampled 10000 times. The RMSE of resampled errors was calculated, and the 10% and 90% percentile of the RMSEs distribution were estimated for the confidence intervals. The results are presented in Fig. 18. The forecast accuracy of temperature improved significantly at all the selected stations when the model resolution increased (grid spacings of 1 and0.25 km) leading to a decrease in RMSE by a maximum 66%. The forecast accuracy of dew point, wind direction and speed improved by a maximum 60% at some stations (e.g., L1D).

4. Conclusions

This study explored the ability of the GEM model to forecast the lake breezes under opposing and non-opposing synoptic flows during the 2015 Pan/Parapan American Games in Toronto. The case studies included the 15 July event where a slow-moving lake-breeze front impacted the GTA lakeshore regions for ~10 hours and the 9 August event where a fast-moving lake-breeze front penetrated more than 60 km inland through the GTA in ~6 hours. The modeled lake breezes were compared with mesoscale analyses, lidar observations of radial winds, and surface stations observations. The following were found:

(i) The GEM model successfully predicted the lake-breeze fronts for the two lake-breeze events. The wind direction shifts to onshore were captured by the model as were the decrease in predicted temperature and increase in dew point.

(ii) The predicted enhanced vertical velocity with GEM 2.5 and 1 km clearly showed the lake-breeze frontal zone for the two events, though the GEM 0.25 km did not produce a clear updraft zone associated with lake-breeze front on 9 August. It seems that the model resolved the large eddies in this case while producing a weak convergence zone associated with lake-breeze front. We speculate that the representation of turbulence in the model contributed to this issue.

(iii) GEM 0.25 km generated elongated, weak updraft structures in the lake breeze inflow region that were approximately aligned with the onshore surface wind for both 15 July and 9 August. This suggests that the high-resolution model likely captured the suppressing effect of the cooler lake air on the generation of thermals.

(iv) Comparisons of the predicted characteristics of lake-breeze fronts including inland penetration, updraft intensity, depth and timing with observations showed that GEM 2.5 km predicted the lake-breeze front characteristics with some degree of accuracy during the two events. However, the accuracy improved significantly when the model ran with the grid point spacings of 0.25 km for the 15 July case and with a grid point spacing of 1 km for the 9 August case.

(v) The model underestimated the cooling behind the lake-breeze front by up to 2.5°C in this study. It also underestimated the rise in dew point by up to 2.1°C. While the increase of model resolution improved the prediction of the temperature drops at all the selected locations, it improved the dew point increases prediction only at some locations. In addition, the model

sometimes failed to capture the sharpness of changes in the wind direction during the passage of the lake-breeze front, possibly due to diffusion processes in the model.

(vi) During the lake-breeze circulation the model underestimated the temperature by up to 3.6°C. While GEM 2.5 km overestimated the dew point by a maximum 3°C, GEM 1 and 0.25 km underestimated the dew point by up to 1.3°C. The GEM 2.5 km model also underestimated the wind speed while the higher-resolution model overestimated by up to 2 ms^{-1}. The biases and variability of errors for wind direction predictions were generally very high.

(vii) During the lake-breeze circulation, the increase of model resolution increased the accuracy of temperature predictions significantly within 90% percentile at all the selected stations. However, it improved the accuracy of dew point, wind speed and direction predictions at some of the selected stations.

There are several aspects of the atmospheric model that need to be examined in order to improve the representation of lake-breeze circulations over the GTA. For instance, how much would better representation of lake surface temperatures improve the GEM's performance? Is the turbulent exchange between the Lake Ontario and the atmosphere correctly simulated? What is the impact of the urban canopy on onshore air temperature, wind speed and lake breezes? The diffusive processes (numerical and physical) might also degrade the quality of the predicted lake breezes. These aspects will be subjects of the future studies.

Acknowledgment:

The authors would like to thank all the participants of the PanAm project including John MacPhee and Reno Sit. Special thanks to Ivan Heckman and Dr. Zhipeng Qu for their assistance with data analysis. Thanks to Brian Greaves for his help with the mesonet plots.

References:

Atkinson, B. W. (1981): Mesoscale Atmospheric Circulations. Academic Press, 495 pp.

Bélair, S., S. Leroyer, N. Seino, L. Spacek, V. Souvanlassy, and D. Paquin-Ricard (2017) : Role and Impact of the Urban Environment in a Numerical Forecast of an Intense Summertime Precipitation Event over Tokyo. *Journal of the Meteorological Society of Japan (under review).*

Bélair, S., L. P. Crevier, J. Mailhot, B. Bilodeau, and Y. Delage (2003a): Operational implementation of the ISBA land surface scheme in the Canadian Regional Weather Forecast Model. Part I: Warm season results. *J. Hydrometeor*., 4, 352–370.

Bélair, S., R. Brown, J. Mailhot, B. Bilodeau, and L. P. Crevier (2003b): Operational implementation of the ISBA land surface scheme in the Canadian Regional Weather Forecast Model. Part II: Cold season results. *J. Hydrometeor*., 4, 371–386.

Biggs, W.G. and M.E. Graves (1962): A Lake Breeze Index. *J. Appl. Meteorol.* **1**:474- 480.

Boodoo, S., D. Hudak, N. Donaldson, and M. Leduc (2010): Application of Dual-Poliarization Radar Melting-Layer Detection Algorithm. J. of Appl. Met. and Clim., 49(8), 1779-1793.

Brasnett, B. (2008): The impact of satellite retrievals in a global seasurface-temperature analysis. *Quart. J. Roy. Meteor. Soc*., 134, 1745–1760.

Charnock, H. (1955): Wind stress over a water surface. *Quart. J. Roy. Meteor*. Soc., 81, 639–640

Comer, N. T. and I. G. McKendry (1993): Observations and numerical modelling of Lake Ontario breezes, *Atmos.-Ocean*, 31, 481-499.

513 Côté, J., S. Gravel, A. Méthot, A. Patoine, M.Roch, and A. Staniforth (1998): The operational
514 CMC–MRB Global Environmental Multiscale (GEM) model. Part I: Design
515 considerations and formulation. *Mon. Wea. Rev*., 126, 1373–1395.

516 Curry, M., J. Hanesiak, S. Kehler, D. Sills and N. Taylor (2016): Ground-based Observations of
517 the Thermodynamic and dynamic properties of lake-breezes in southern Manitoba,
518 Canada. *Boundary Layer Meteorol*.

519 Darby, L. S., W. D. Neff, and R. M. Banta (1999): Multiscale analysis of a meso-β frontal
520 passage in the complex terrain of the Colorado Front Range. *Mon. Wea. Rev*., 127, 2062-
521 2081.

522 Deacu, D., V. Fortin, E. Klyszejko, C. Spence, and P. D. Blanken (2012): Predicting the net
523 basin supply to the Great Lakes with a hydrometeorological model. *J. Hydrometeor*., 13,
524 1739–1759.

525 DiCiccio, T.J. and B. Efron, (1996): Bootstrap confidence intervals (with discussion), *Statistical*
526 *Science*, 11, 189–228.

527 Dupont, F., Chittibabu, P., Fortin, V., Rao, Y. R., and Lu, Y.: Assessment of a NEMO-based
528 hydrodynamic modelling system for the Great Lakes (2012): *Water Qual. Res. J. Can*.,
529 47, 198–214.

530 Estoque, M.A., J. Gross and H.W. Lai (1976): A Lake Breeze over Southern Lake Ontario. *Mon.*
531 *Wea. Rev.* 104, 386-396.

532 Estoque, M.A. and J.M. Gross (1981): Further Studies of a Lake Breeze Part II: Theoretical
533 Study. *Mon. Wea. Rev.* 109, 619-634.

534 Fillion L, Tanguay M, Lapalme E, Denis B, Desgagne M, Lee V, Ek N, Liu Z, Lajoie M, Caron
535 J-F, Pag´e C. (2010): The Canadian regional data assimilation and forecasting system.
536 *Weather and Forecasting*, 25, 1645-1669.

537 Girard, C., A. Plante, M. Desgagné, R. McTaggart-Cowan, J. Côté, M. Charron, S. Gravel, V.
538 Lee, A. Patoine, A. Qaddouri, M. Roch, L. Spacek, M. Tanguay, P.A. Vaillancourt, and
539 A. Zadra, (2014): Staggered Vertical Discretization of the Canadian Environmental
540 Multiscale (GEM) Model Using a Coordinate of the Log-Hydrostatic-Pressure Type.
541 *Mon.Wea.Rev*, 142, 1183-1196.

542 Hanna, S. R. (1994): Mesoscale meteorological model evaluation techniques with emphasis on
543 needs of air quality models. *Mesoscale Modeling of the Atmosphere, Meteor. Monogr.*,
544 No. 47, Amer. Meteor. Soc., 47–62.

545 Harris, L. and V. R. Kotamarthi (2005): The characteristics of the Chicago Lake breeze and its
546 effects on trace particle transport: results from an episodic event simulation. *J Appl*
547 *Meteorol* 44, 1637–1654

548 Hastie, D. R., J. Narayan, C. Schiller, H. Niki, P. B. Shepson, D. M. L. Sills, P. A. Taylor, Wm.
549 J. Moroz, J. W. Drummond, N. Reid, R. Taylor, P. B. Roussel and O. T. Melo (1999):
550 Observational evidence for the impact of lake breeze circulation on ozone concentrations
551 in southern Ontario. *Atmospheric Environment*, 33, 323-335

552 Hayden, K.L., D.M.L. Sills, J.R. Brook, S.M. Li, P.A. Makar, M.Z. Markovic, P. Liu, K.G.
553 Anlauf, J.M. O'Brien, Q. Li and R. McLaren (2011): Aircraft study of the impact oflake-
554 breeze circulations on trace gases and particles during BAQS-Met 2007. *Atmos. Chem.*
555 *Phys*. 11, 10173e10192.

556 Hudak, D., P. Rodriguez, G. Lee, A. Ryzhkov, F. Fabry, and N. Donaldson (2006): Winter
557 precipitation studies with a dual polarized C-band radar. Preprints, Fourth European
558 Conf. on Radar in Meteorology and hydrology (ERAD 2006), Barcelona, Spain, Servei
559 Meteorologic de Catalunya, 9-12.

560 Joe, P., S. Bélair, N.B. Bernier, J.R. Brook, D. Brunet, V. Bouchet, W. Burrows, J.P. Charland,
561 A. Dehghan, N. Driedger, C. Duhaime, G. Evans, R. Frenette, I. Gultepe, D. Henderson,
562 A. Herdt, N. Hilker, L. Huang, E. Hung, G. Isaac, D. Johnston, C.-H. Jeong, J. Klaassen,
563 S. Leroyer, H. Lin, M. MacDonald, J. MacPhee, Z. Mariani, J. Reid, A. Robichaud, Y.
564 Rochon, D. Sills, K. Shairsingh, C. Stroud, Y. Su, N. Taylor, J.M. Wang, J. Vanos, J.
565 Voogt, T. Wiechers, S. Wren, H. Yang, and T. Yip (2017): The Pan-American Games
566 Science Showcase Project. *Amer. Meteor. Soc*., doi: 10.1175/BAMS-D-16-0162.1.

567 Keen, C.S. and W.A. Lyons, (1978): Lake/Land Breeze Circulations on the Western Shore of
568 Lake Michigan. *J. Appl. Meteorol.* 17, 1843-1855.

569 Kehler, S., J. Hanesiak, M. Curry, D. Sills and N. Taylor, (2016): High resolution Deterministic
570 Prediction System (HRDPS) simulations of Manitoba lake breezes, *Atmos. Ocean.*54, 93-
571 107.

572 King, P. W. S., M. Leduc, D. M. L. Sills, N. R. Donaldson, D. R. Hudak, P. I. Joe, and B. P.
573 Murphy (2003): Lake breezes in Southern Ontario and their relation to tornado
574 climatology. *Weather and Forecasting*, 18, 795-807.

575 Leroyer, S., J. Mailhot, S. Bélair, A. Lemonsu, and I. Strachan, (2010): Modeling the surface
576 energy budget during the thawing period of the 2006 Montreal Urban Snow Experiment.
577 *J. Appl. Meteor. Climatol.*, **49,** 68–84.

578 Leroyer, S., S. Bélair, J. Mailhot, and I. Strachan, (2011): Microscale numerical prediction over
579 Montreal with the Canadian external urban modeling system. J. Appl. Meteor. Climatol.,
580 50, 2410–2428.

581 Leroyer, S., S. Bélair, S.Z. Husain and J. Mailhot, Subkilometer Numerical Weather Prediction
582 in an Urban Coastal Area: A Case Study over the Vancouver Metropolitan Area, (2014):
583 Subkilometer Numerical Weather Prediction in an Urban Coastal Area: A Case Study
584 over the Vancouver Metropolitan Area, *J. Appl. Meteorol. Clim.*, 53, 1433-1453.

585 Lyons, W.A. (1972): The Climatology and Prediction of the Chicago Lake Breeze. *J. Appl.*
586 *Meteorol*., 11, 1259-1270.

587 Mariani, Z., A. Dehghan, P. Joe, D. Sills (2017): Observations of lake breeze events during the
588 Toronto 2015 Pan/Parapan American Games. *Boundary Layer Meteorol*., DOI
589 10.1007/s10546-017-0289-3.

590 Mason, P. J., and A. R. Brown (1999): On subgrid models and filter operations in large eddy
591 simulations. *J.Atmos. Sci*., 56, 2101–2114,

592 Milbrandt, J. A., and M. K. Yau (2005): A multimoment bulk microphysics parameterization.
593 Part I: Analysis of the role of the spectral shape parameter. *J. Atmos. Sci*., 62, 3051–3064

594 Noilhan, J., and S. Planton (1989): A simple parameterization of land surface processes for
595 meteorological models. *Mon. Wea. Rev*., 117, 536–549.

596 Pielke, R. A. (1984): Mesoscale Meteorological Modeling. Academic Press, 612 pp.

597 Sills, D., P. Taylor, P. King, W. Hocking and I. Nichols (2002): ELBOW 2001 - studying the
598 relationship between lake breezes and severe weather: project overview and preliminary

599 results. *Preprints, 21st Severe Local Storms Conference*, San Antonio, TX, *Amer.*
600 *Meteorol. Soc.*, 611-614.

601 Sills, D. M. L., J. R. Brook, I. Levy, P. A. Makar, J. Zhang, and P. A. Taylor (2011): Lake
602 breezes in the southern Great Lakes region and their influence during BAQS-Met 2007.
603 *Atmos. Chem. Phys.*, 11, 7955-7973.

604 Tsunematsu, N., H. Iwai, S. Ishii, Y. Murayama, M. Yasui, and K. Mizutani (2009): The
605 Formation of Sharp Multi-Layered Wind Structure over Tokyo Associated with Sea-
606 breeze Circulation. SOLA, 5, 1-4.

607 Wentworth, G.R., J.G. Murphy, and D.M.L. Sills (2015): Impact of lake breezes on ozone and
608 nitrogen oxides in the Greater Toronto Area. *Atmos. Env*., 109, 52-60.

609 Wilson, J. W., T. M. Weckwerth, J. Vivekanandan, R. M. Wakimoto, and R. W. Russell (1994):
610 Boundary Layer Clear-Air Radar Echoes: Origin of Echoes and Accuracy of Derived
611 Winds. Atmos. Ocean. Technol, 11, 1184-1206.

612 Zadra, A., D. Caya, J. Cote, B. Dugas, C. Jones, R. Laprise, K. Winger, and L.-P. Caron (2008):
613 The next Canadian regional climate model. *Phys. Canada*, 64, 75–83.

614

615

616

Figures Captions

Fig. 1. The GEM domains.

Fig. 2. Mesonet analyses (a) on 15 July at 2000 UTC, (b) on 9 August at 1600 UTC. The meteorological data including wind barbs and the radar reflectivity are shown. The locations of lake-breeze fronts are indicated by the magenta lines. Note that the lake-breeze fronts at the top of the Fig. 2a are generated by Lake Simcoe and Georgian Bay.

Fig. 3. The GEM 0.25 km numerical output for the lake-breeze event of 15 July at 2000 UTC, 2015. Plots of (a) vertical velocity (ms^{-1}) at ~120 m AGL, (b) horizontal wind speed (ms^{-1}) and direction ($^{\circ}$) at ~10 m AGL, (c) temperature ($^{\circ}C$) and (d) dew point ($^{\circ}C$) at ~5 m AGL. The plots cover an area of ~50×30 km^2. The white and magenta lines represent the GTA lakeshores and the lake-breeze front determined by the mesoscale analyses, respectively. The red line indicates the cross-section passing through the selected surface stations in Table 2. Hanlan's Point and Highway 400 ONroute are the locations of the lidars, and Z2D is the location of the surface station at the lakeshore.

Fig. 4. Same as Fig. 3, except for 9 August, 2015 at 1600 UTC.

Fig. 5. vertical velocity (ms^{-1}) along the shore-A2T cross-section at ~120 m AGL with (a) GEM 2.5 km, (b) GEM 1 km and (c) GEM 0.25 km on 15 July. The white dots indicate the inland penetration of lake-breeze front as given by mesonet analysis. The location of the cross-section in the GTA is shown in Fig. 3a. Note that figures are plotted using different scales to clearly show the updraft zone.

Fig. 6. The same as Fig. 5, except for 9 August, 2015

638 Fig. 7. Horizontal velocity (ms^{-1}) along the shore-A2T cross-section with GEM 0.25 km on 9
639 August. A vector pointing right to left is a northerly flow.

640 Fig. 8. Locations of the modeled and observed lake-breeze front along the shore-A2T cross-
641 section (red line in Figs. 3a and 4a) on (a) 15 July and (b) 9 August. Note that the predicted lake
642 breeze with GEM 0.25 km has passed by A2T station by 1700 UTC on 9 August.

643 Fig. 9. Vertical velocity in ms^{-1} (a) measured by lidar at Hanlan's Point from 1400 UTC on 15
644 July until 0000 UTC on 16 July, and the predicted vertical velocities (ms^{-1}) at the nearest grid
645 point to Hanlan's Point for the same period with (b) GEM 2.5 km, (c) GEM 1 km and (d) GEM
646 0.25 km. The white color indicates no measurements. Note that figures are plotted using different
647 scales to clearly show the updraft zone, however the scales for (a) and (d) are the same.

648 Fig. 10. A snapshot of lidar measurements of radial velocity in ms^{-1} (PPI scan) when the lake-
649 breeze front was passing over (a) Hanlan's Point on 15 July at 1424 UTC and (b) Highway 400
650 ONroute on 9 August at 1827 UTC. Negative (blue) velocities represent winds towards the lidar
651 (onshore); positive (red) velocities represent winds away from the lidar (offshore).

652 Fig. 11. The same as Fig. 9 except at Highway 400 ONroute from 1400 UTC until 2100 UTC on
653 9 August. The arrow shows the time and the location of the maximum vertical velocity for the
654 available lidar measurements.

655 Fig. 12. Lidar measurements of vertical velocity from 1800 UTC to 1830 UTC at the height
656 range from 60 to 240 m AGL at Highway 400 ONroute. The maximum vertical velocity occurred
657 at 1819 UTC for the measurements below 240 m AGL.

Fig. 13. A snapshot of lidar measurements of radial velocity in ms^{-1} (RHI scan) when the lake-breeze front was passing over (a) Hanlan's Point on 15 July at 1445 UTC (b) Highway 400 ONroute on 9 August at 1815 UTC. Negative (blue) velocities represent winds towards the lidar; positive (red) velocities represent winds away from the lidar. The direction of the x-axis is facing south.

Fig. 14. Observed and predicted lake-breeze depths using lidar and GEM at intervals of 15 minutes at (a) Hanlan's Point on 15 July and (b) Highway 400 ONroute on 9 August. Note that the lake-breeze front arrived at Hanlan's Point and Highway 400 ONroute approximately at 1424 UTC and 1815 UTC, respectively. The modeled depths were estimated at the nearest grid point to the lidar sites.

Fig. 15. Comparisons of observations with the model output at the nearest grid point to Z2D station from the period of 1200 UTC on 15 July to 0115 UTC on 16 July, 2015. (a) temperature ($^{\circ}$C), (b) dew point ($^{\circ}$C), (c) horizontal wind direction ($^{\circ}$) and (d) horizontal wind speed (ms^{-1}). The observed lake-breeze front arrived at 1508 UTC. The temporal resolution of observations and predictions are 1 and 15 minutes, respectively.

Fig. 16. The same as Fig. 15 except from 1200 UTC on 9 August to 0000 UTC on 10 August at L1F station. The lake-breeze front arrived at 1643 UTC.

Fig. 17. The MBE values for (a) temperature ($^{\circ}$C), (b) dew point ($^{\circ}$C), (c) wind direction ($^{\circ}$) and (d) wind speed (ms^{-1}) at the nearest grid point to surface stations for the periods of time that surface stations were affected by the lake-breeze circulations on 15 July and 9 August. The error bars represents the STDE values.

679 Fig. 18. The RMSE values and corresponding 10% and 90% confidence intervals for (a)
680 temperature ($^{\circ}$C), (b) dew point ($^{\circ}$C), (c) wind direction ($^{\circ}$) and (d) wind speed (ms^{-1}) at the
681 nearest grid point to surface stations for the periods of time that surface sites were affected by the
682 lake-breeze circulations on 15 July and 9 August, 2015.

683 Fig. A1. Hourly mesonet analyses for 15 July, 2015.

684 Fig. A2. The same as Fig. A1 except for 9 August, 2015.
685

686

687

688

689

690

691

692

693

694

Table 1. Selected surface stations.

Surface sites	Latitude	Longitude	Type	Height of sensors from ground (m)
Z2D	43°38'22.3"N	79°20'53.7"W	Compact/ground	2.5
L1B	43°40'41.5"N	79°26'34.6"W	Compact/rooftop	10.3
L1C	43°41'56.2"N	79°27'5.7"W	Compact/rooftop	9.1
L1D	43°43'7.1"N	79°28'7.4"W	Compact/rooftop	4
L1E	43°44'51.8"N	79°28'47.6"W	Compact/rooftop	9.1
L1F	43°49'3.2"N	79°31'24.2"W	Compact/rooftop	7.3
A2T	43°51'47.7"N	79°32'28.9"W	Tower/ground	10 (wind) 1.5 (temperature and dew point)

Table 2. RDPS and GEM configurations.

Domains	RDPS	Domain 1 (nested)	Domain 2 (nested)	Domain 3 (nested)
Horizontal grid spacing (km)	10	2.5	1	0.25
Number of grid points	360×256	512x512	512x512	1024×1024
Vertical momentum levels	58	57	57	57
Levels below 500 m	6	15	15	15
Levels below 1500 m	13	26	26	26
Time steps (s)	450	60	30	12
Land surface model (URB)	ISBA	ISBA	ISBA+TEB	ISBA+TEB
Land surface model (VEG)	ISBA	ISBA	ISBA	ISBA
Planetary Boundary Layer	MoisTKE	MoisTKE	MoisTKE	MoisTKE
Microphysics	ConSun	MY-DM	MY-DM	MY-DM

Table 3. Temperature drops, T, dew point rises, Td, and wind shift timings due to lake-breeze front at selected surface stations. The n/a for Td means highly variable measurements. Also when the wind shift to onshore was not observed, n/a was recoreded for the timing. Zero means no decrease in temperature (or increase in dew point) was occurred.

		observations			GEM 2.5 km			GEM 1 km			GEM 0.25 km		
Day	Station	T↓ (˚C)	Td↑ (˚C)	Time (UTC)	T↓ (˚C)	Td↑ (˚C)	Time (UTC)	T↓ (˚C)	Td↑ (˚C)	Time (UTC)	T↓ (˚C)	Td↑ (˚C)	Time (UTC)
Jul15	Z2D	1.3	1.6	1508	0.9	0	1630	0.7	0.7	1615	0	0.6	1615
Jul15	L1B	2.3	3	1845	0	3	n/a	0	0.6	n/a	0.4	1.6	n/a
Aug9	Z2D	1.4	1.1	1442	0.2	0.3	1615	0	0.3	1600	0	0.3	1600
Aug9	L1B	1.1	n/a	1445	0	0	1445	0.1	0	1445	0.2	0.9	1445
Aug9	L1C	1.1	n/a	1510	0	0	1445	0.2	0	1530	0.2	1	1515
Aug9	L1D	1.6	1.3	1548	0	0	1515	0.5	0.8	1545	0	1	1515
Aug9	L1E	1.2	n/a	1630	0	0	1415	0.2	0.9	1615	0.4	0.7	1500
Aug9	L1F	1.5	2.1	1643	0	0	1445	0.2	0.4	1600	0.3	1	1615
Aug9	A2T	2.5	n/a	1738	0	0.2	1645	0	0.9	1700	0	2.5	1600

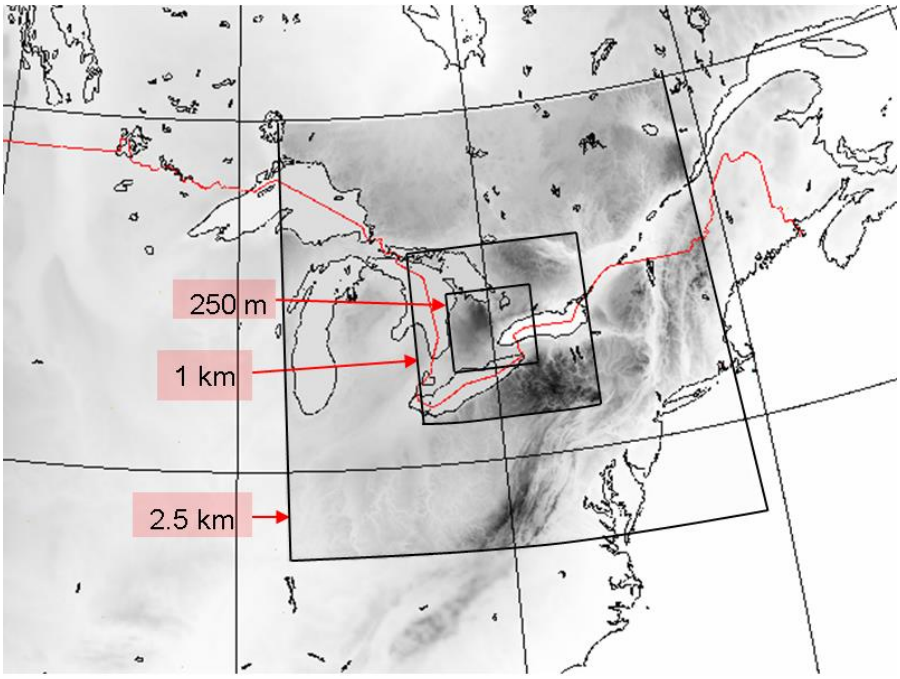

Fig. 1. The GEM domains.

(a)

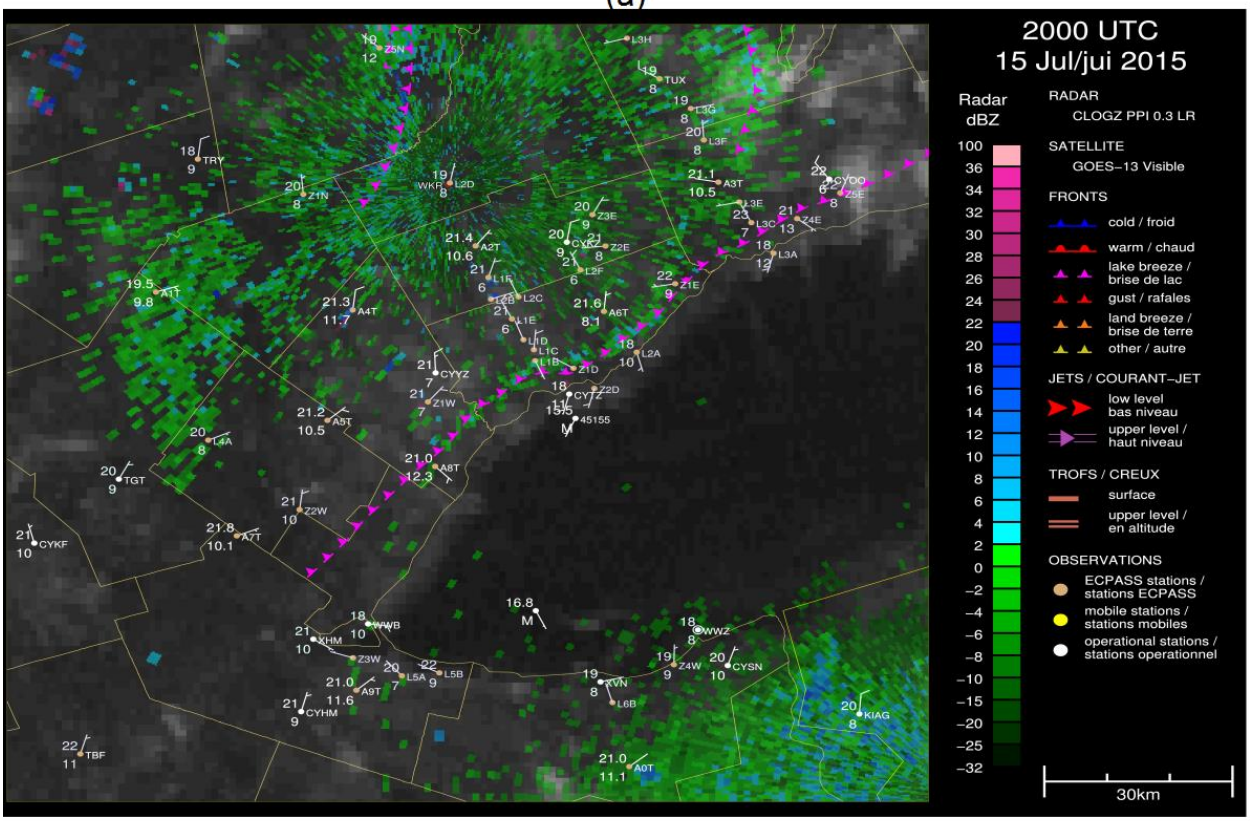
2000 UTC
15 Jul/jui 2015
Radar dBZ
RADAR
CLOGZ PPI 0.3 LR
SATELLITE
GOES–13 Visible
FRONTS
cold / froid
warm / chaud
lake breeze / brise de lac
gust / rafales
land breeze / brise de terre
other / autre
JETS / COURANT–JET
low level bas niveau
upper level / haut niveau
TROFS / CREUX
surface
upper level / en altitude
OBSERVATIONS
ECPASS stations / stations ECPASS
mobile stations / stations mobiles
operational stations / stations operationnel
100 36 34 32 30 28 26 24 22 20 18 16 14 12 10 8 6 4 2 0 −2 −4 −6 −8 −10 −15 −20 −25 −32
30km

(b)

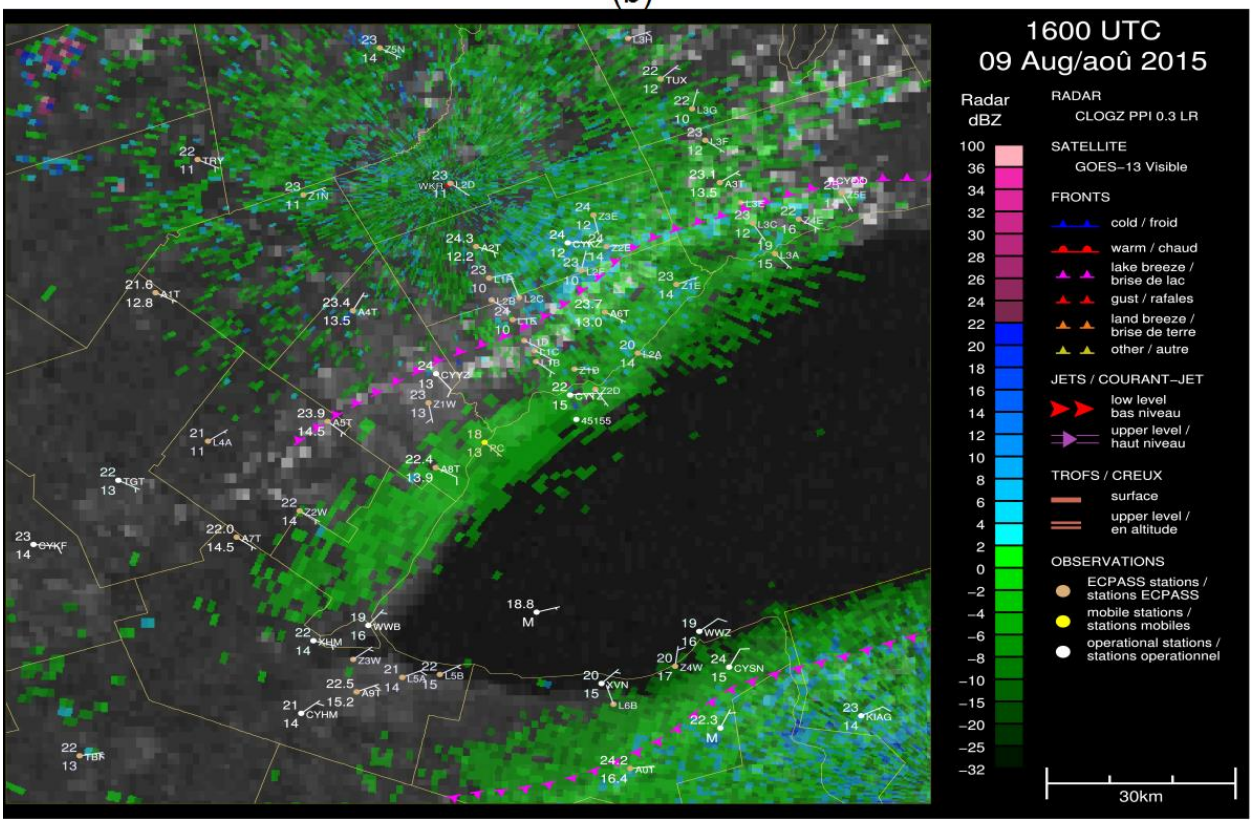
1600 UTC
09 Aug/aoû 2015
Radar dBZ
RADAR
CLOGZ PPI 0.3 LR
SATELLITE
GOES–13 Visible
FRONTS
cold / froid
warm / chaud
lake breeze / brise de lac
gust / rafales
land breeze / brise de terre
other / autre
JETS / COURANT–JET
low level bas niveau
upper level / haut niveau
TROFS / CREUX
surface
upper level / en altitude
OBSERVATIONS
ECPASS stations / stations ECPASS
mobile stations / stations mobiles
operational stations / stations operationnel
100 36 34 32 30 28 26 24 22 20 18 16 14 12 10 8 6 4 2 0 −2 −4 −6 −8 −10 −15 −20 −25 −32
30km

712

Fig. 2. Mesonet analyses (a) on 15 July at 2000 UTC, (b) on 9 August at 1600 UTC. The meteorological data including wind barbs and the radar reflectivity are shown. The locations of lake-breeze fronts are indicated by the magenta lines. Note that the lake-breeze fronts at the top of the Fig. 2a are generated by Lake Simcoe and Georgian Bay.

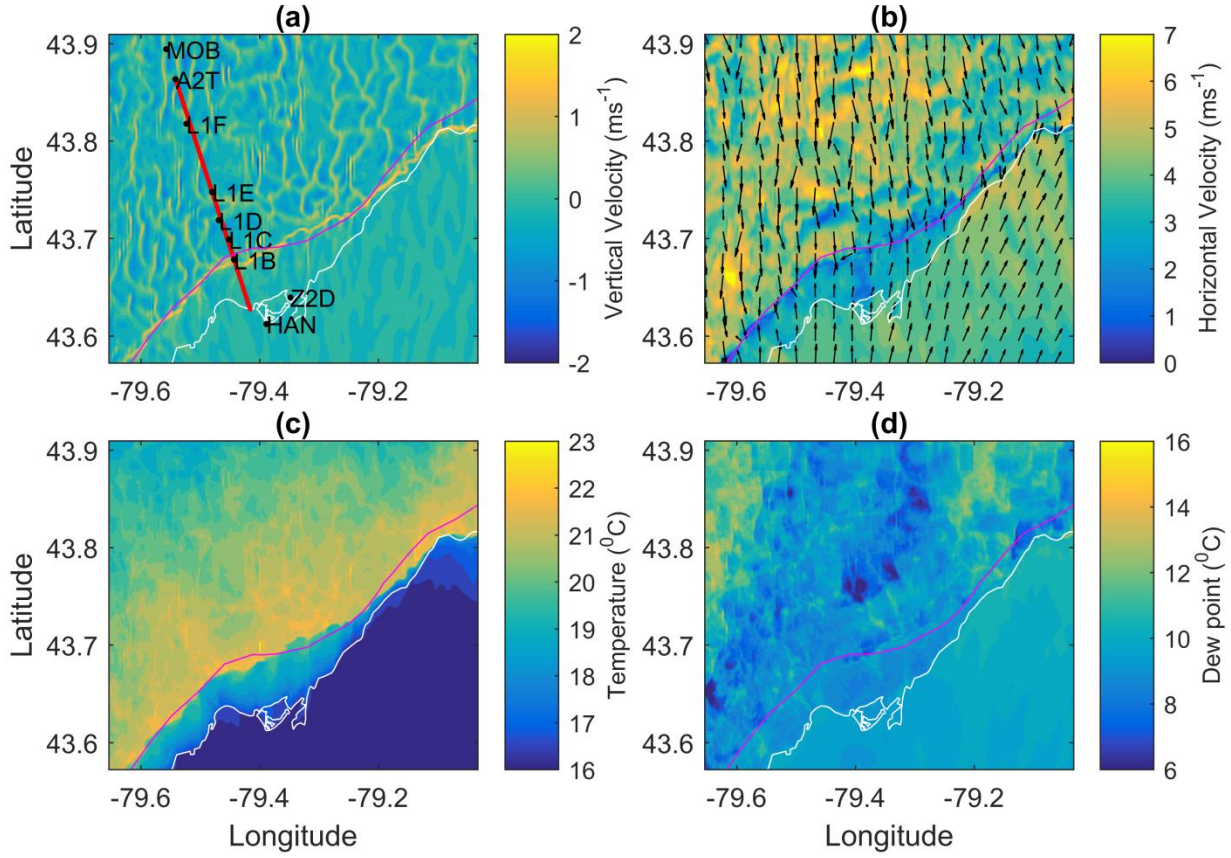

Fig. 3. The GEM 0.25 km numerical output for the lake-breeze event of 15 July at 2000 UTC, 2015. Plots of (a) vertical velocity (ms^{-1}) at ~120 m AGL, (b) horizontal wind speed (ms^{-1}) and direction ($^{\circ}$) at ~10 m AGL, (c) temperature ($^{\circ}C$) and (d) dew point ($^{\circ}C$) at ~5 m AGL. The plots cover an area of ~50×30 km^2. The white and magenta lines represent the GTA lakeshores and the lake-breeze front determined by the mesoscale analyses, respectively. The red line indicates the cross-section passing through the selected surface stations in Table 2. Hanlan's Point and

725 Highway 400 ONroute are the locations of the lidars, and Z2D is the location of the surface
726 station at the lakeshore.

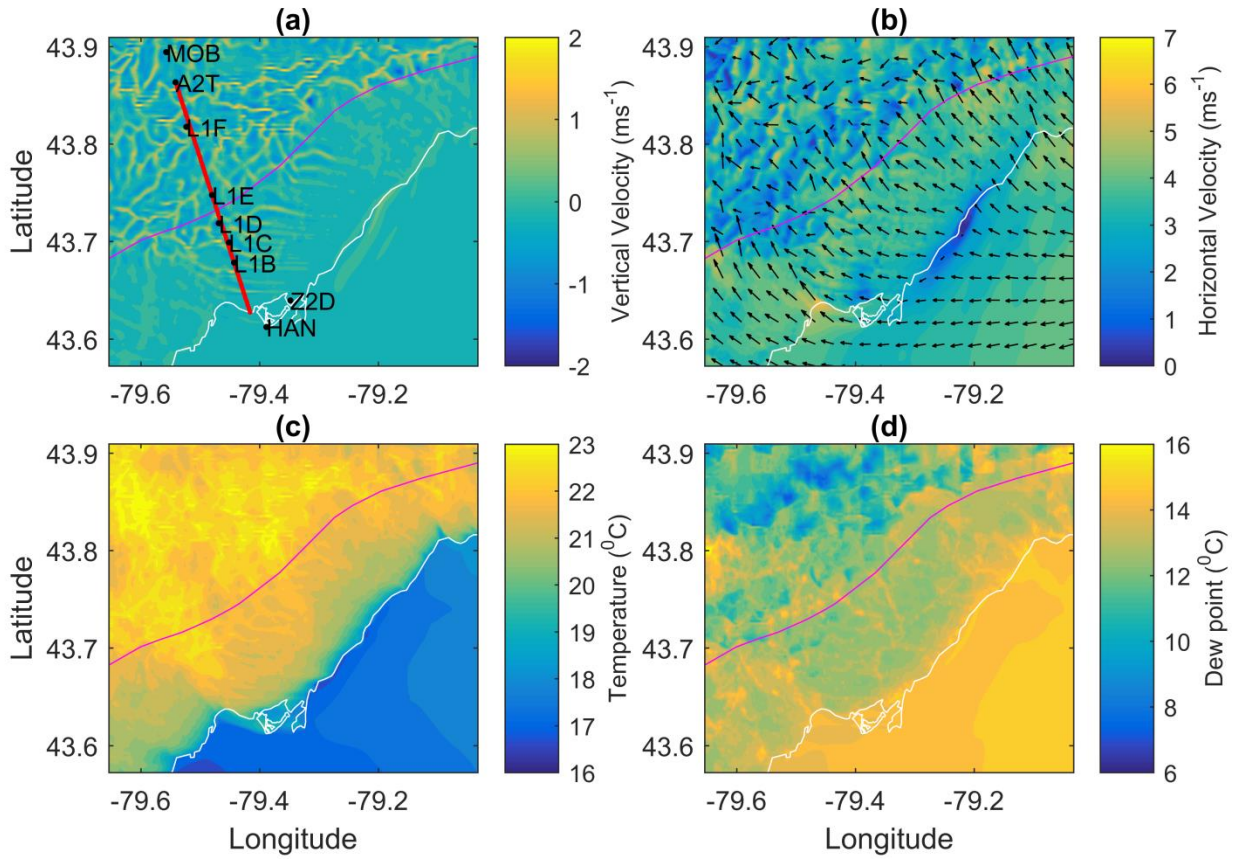

727

728 Fig. 4. Same as Fig. 3, except for 9 August, 2015 at 1600 UTC.

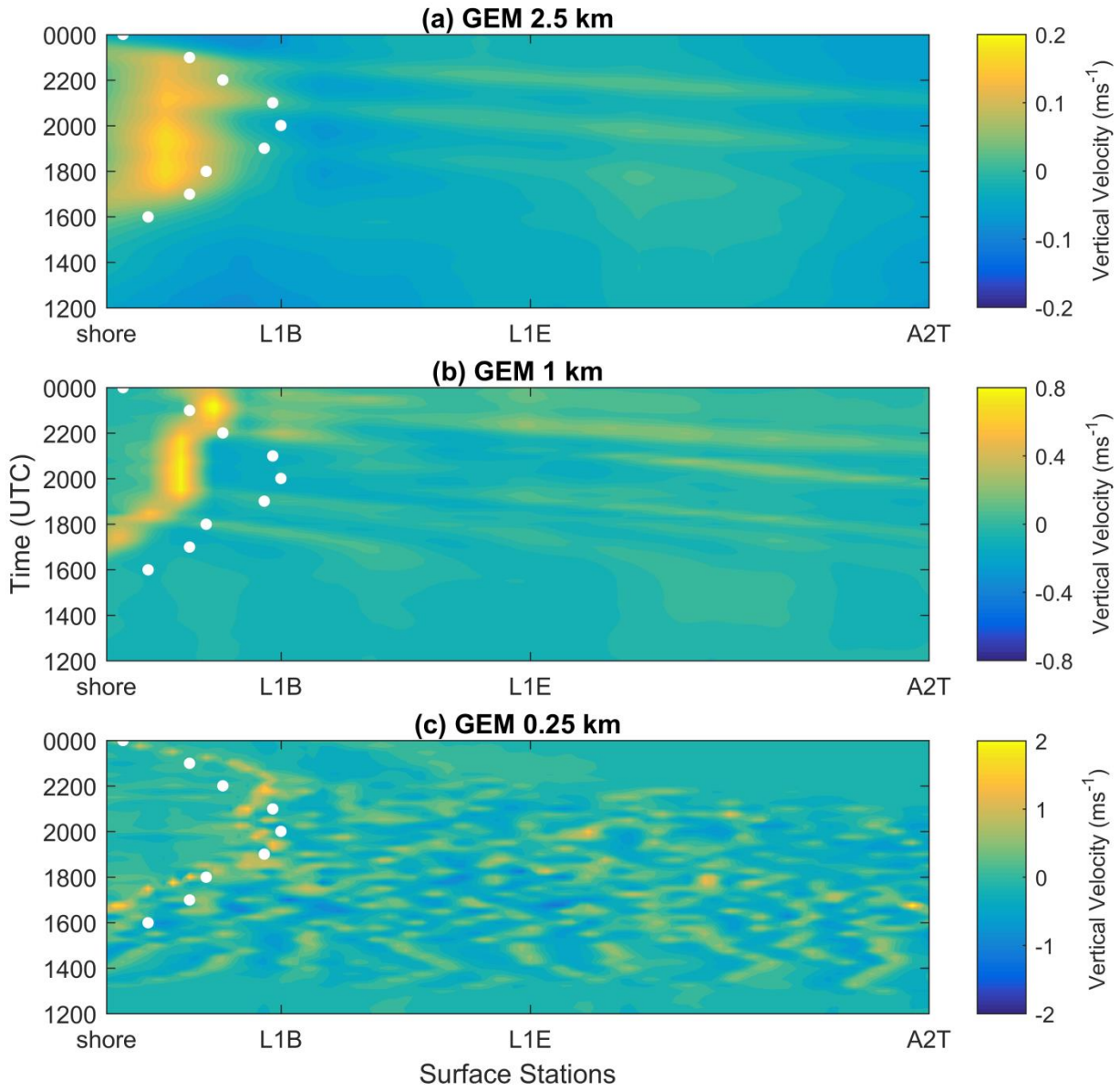

729

730 Fig. 5. vertical velocity (ms^{-1}) along the shore-A2T cross-section at ~120 m AGL with (a) GEM
731 2.5 km, (b) GEM 1 km and (c) GEM 0.25 km on 15 July. The white dots indicate the inland
732 penetration of lake-breeze front as given by mesonet analysis. The location of the cross-section
733 in the GTA is shown in Fig. 3a. Note that figures are plotted using different scales to clearly
734 show the updraft zone.

735

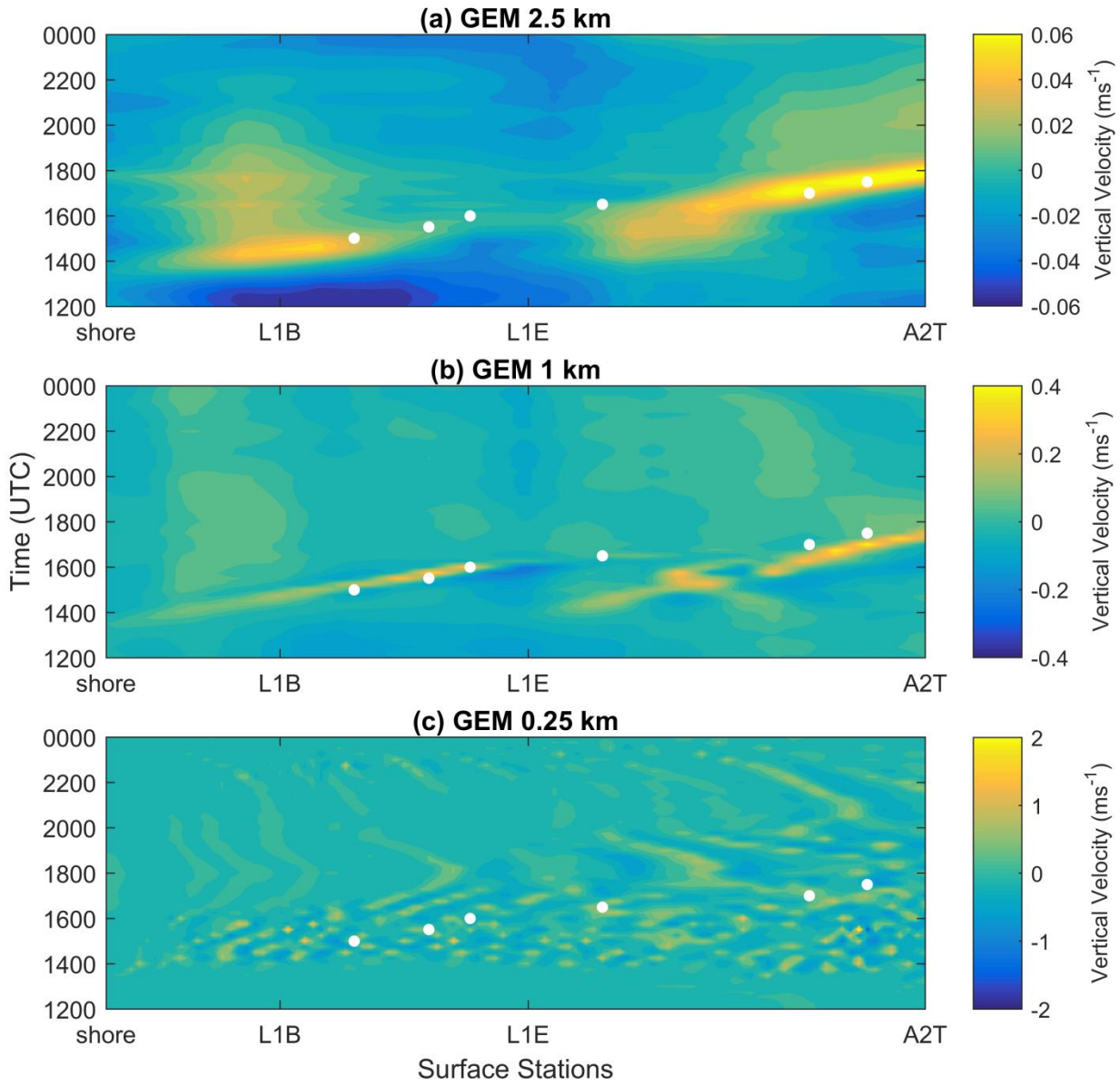

736

737 Fig. 6. The same as Fig. 5, except for 9 August, 2015

738

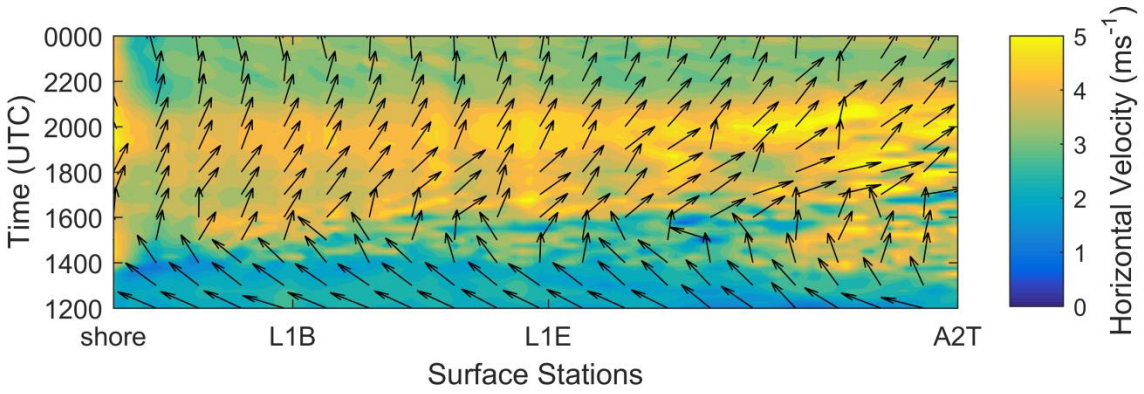

739

740 Fig. 7. Horizontal velocity (ms^{-1}) along the shore-A2T cross-section with GEM 0.25 km on 9

741 August. A vector pointing right to left is a northerly flow.

742

743

744

745

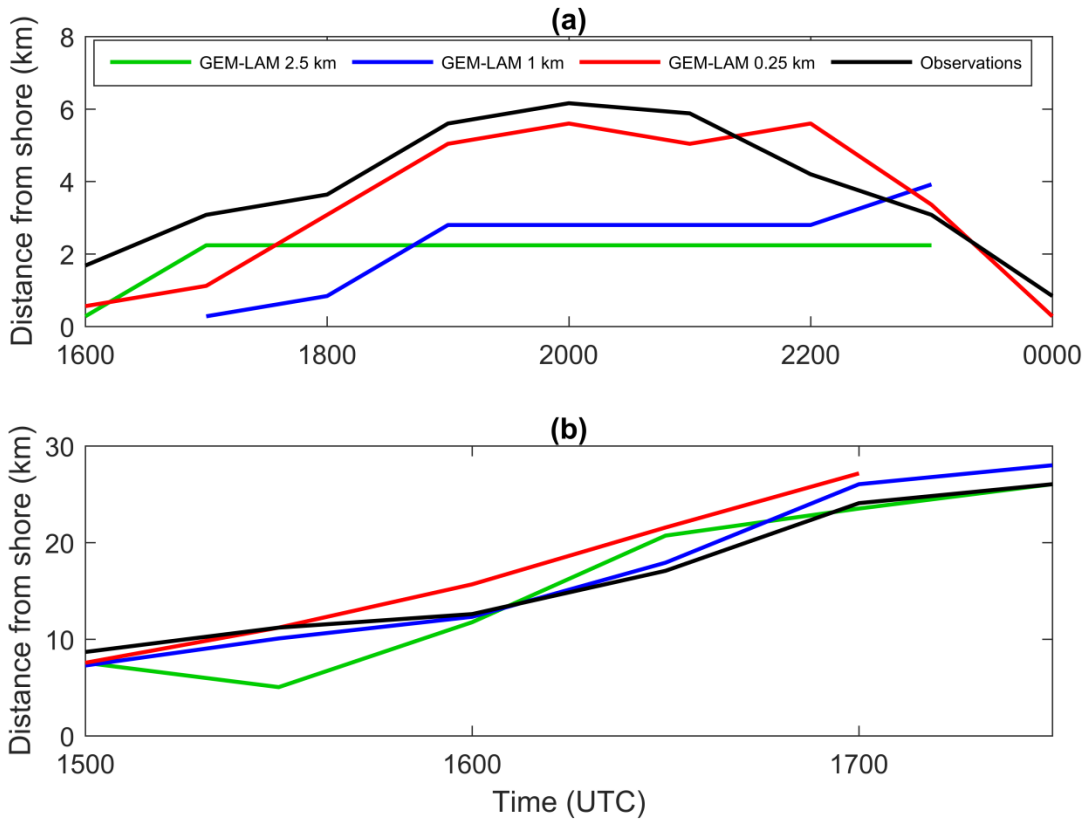

746

747 Fig. 8. Locations of the modeled and observed lake-breeze front along the shore-A2T cross-
748 section (red line in Figs. 3a and 4a) on (a) 15 July and (b) 9 August. Note that the predicted lake
749 breeze with GEM 0.25 km has passed by A2T station by 1700 UTC on 9 August.

750

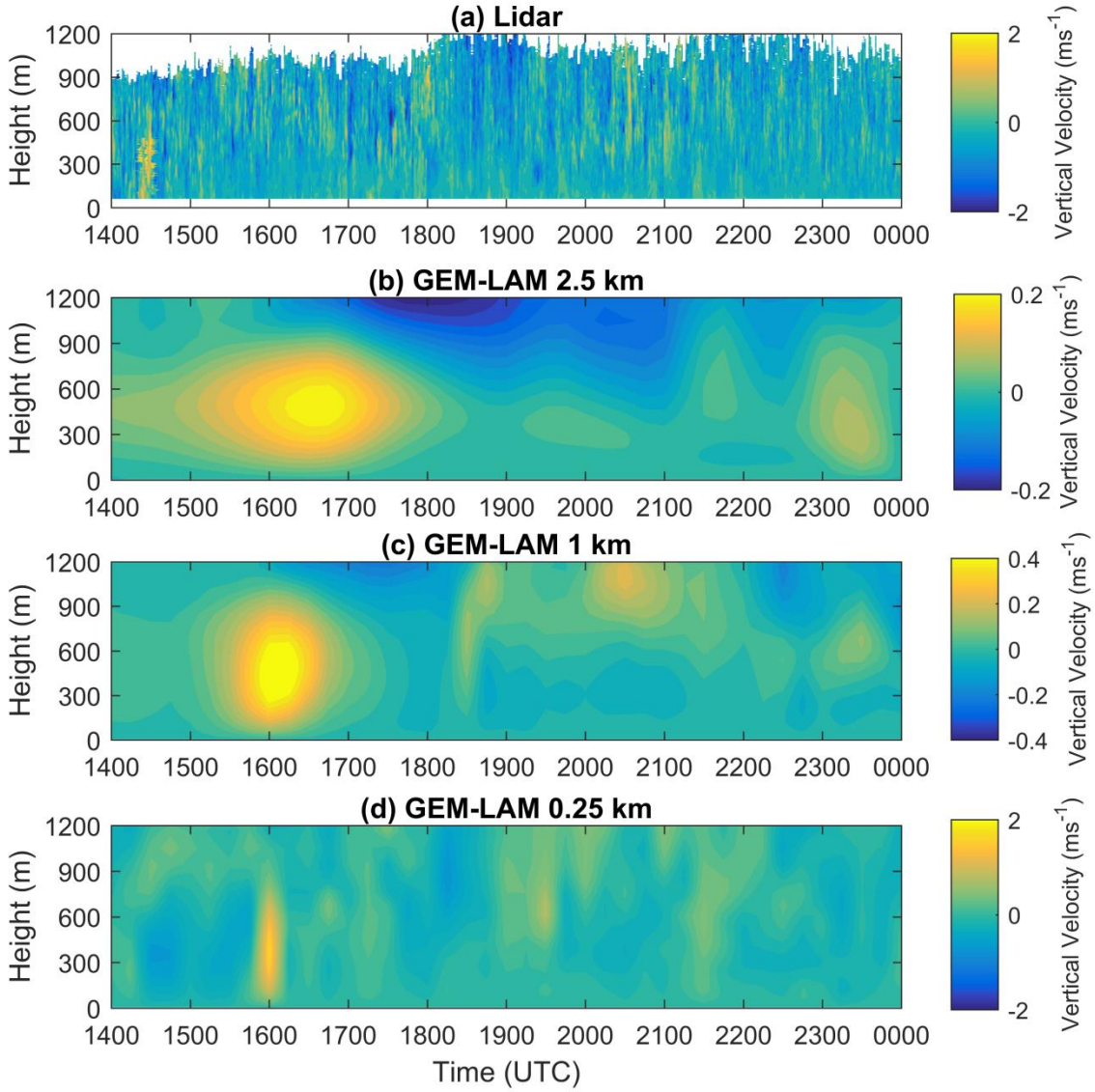

751

752 Fig. 9. Vertical velocity in ms^{-1} (a) measured by lidar at Hanlan's Point from 1400 UTC on 15
753 July until 0000 UTC on 16 July, and the predicted vertical velocities (ms^{-1}) at the nearest grid
754 point to Hanlan's Point for the same period with (b) GEM 2.5 km, (c) GEM 1 km and (d) GEM
755 0.25 km. The white color indicates no measurements. Note that figures are plotted using different
756 scales to clearly show the updraft zone, however the scales for (a) and (d) are the same.

757

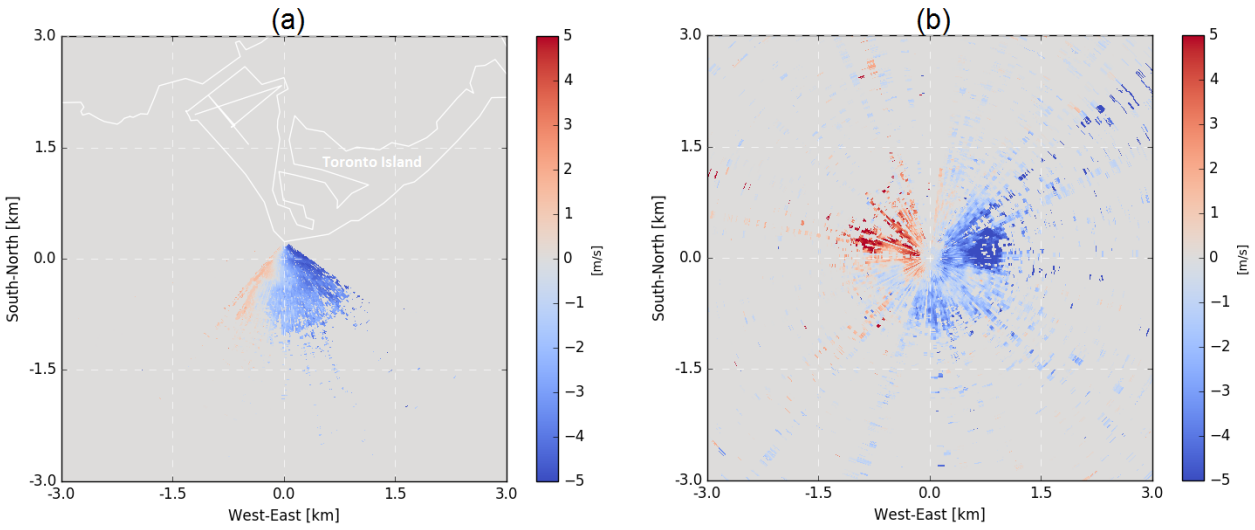

Fig. 10. A snapshot of lidar measurements of radial velocity in ms^{-1} (PPI scan) when the lake-breeze front was passing over (a) Hanlan's Point on 15 July at 1424 UTC and (b) Highway 400 ONroute on 9 August at 1827 UTC. Negative (blue) velocities represent winds towards the lidar (onshore); positive (red) velocities represent winds away from the lidar (offshore).

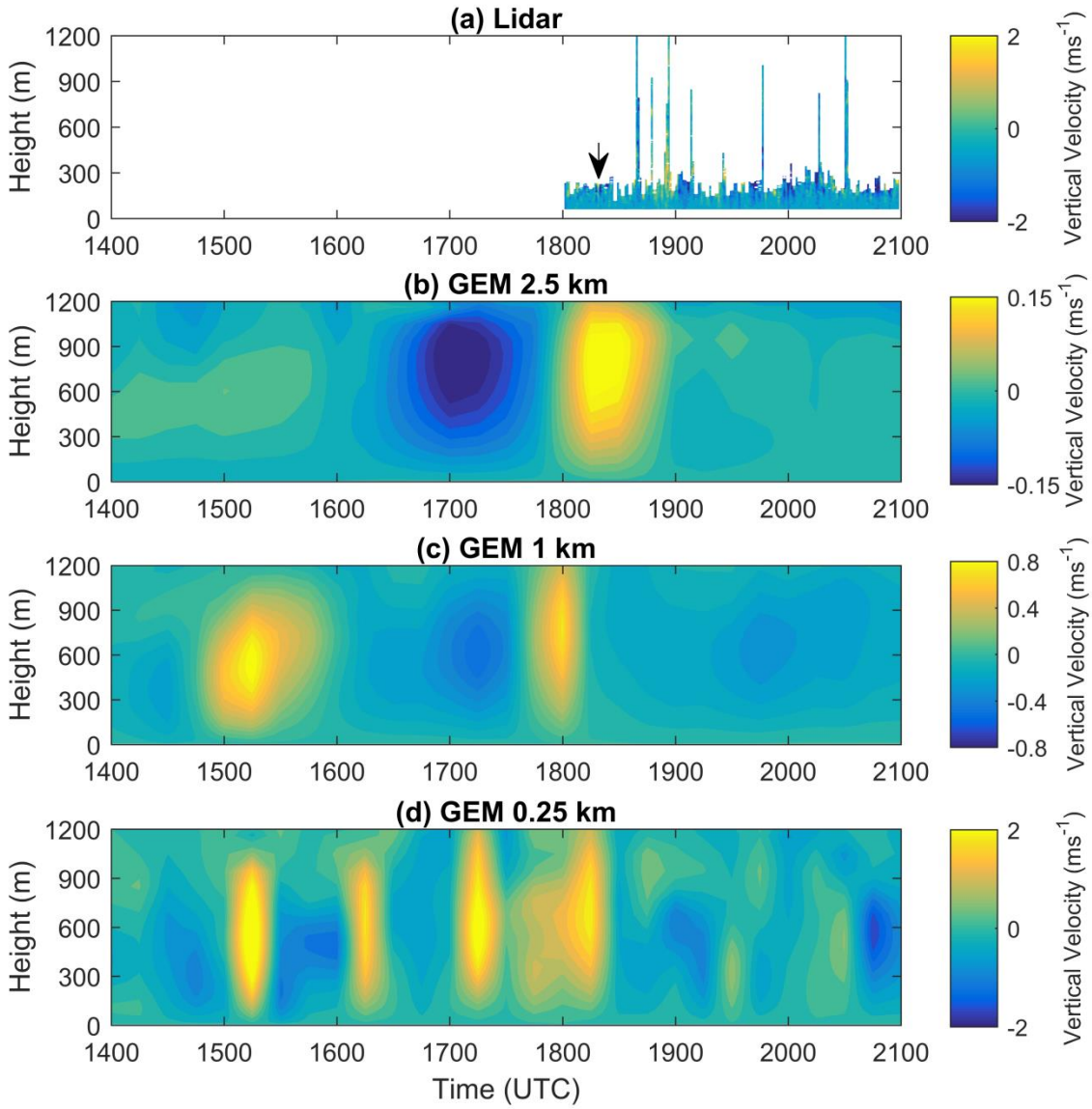

763

764 Fig. 11. The same as Fig. 9 except at Highway 400 ONroute from 1400 UTC until 2100 UTC on
765 9 August. The arrow shows the time and the location of the maximum vertical velocity for the
766 available lidar measurements.

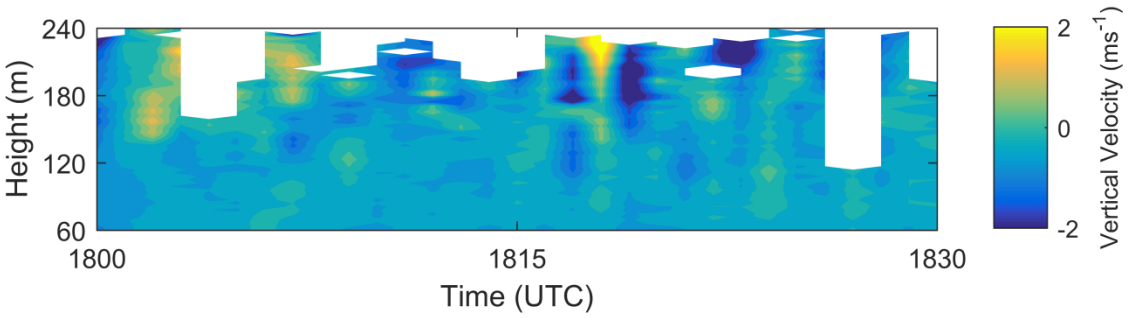

Fig. 12. Lidar measurements of vertical velocity from 1800 UTC to 1830 UTC at the height range from 60 to 240 m AGL at Highway 400 ONroute. The maximum vertical velocity occurred at 1819 UTC for the measurements below 240 m AGL.

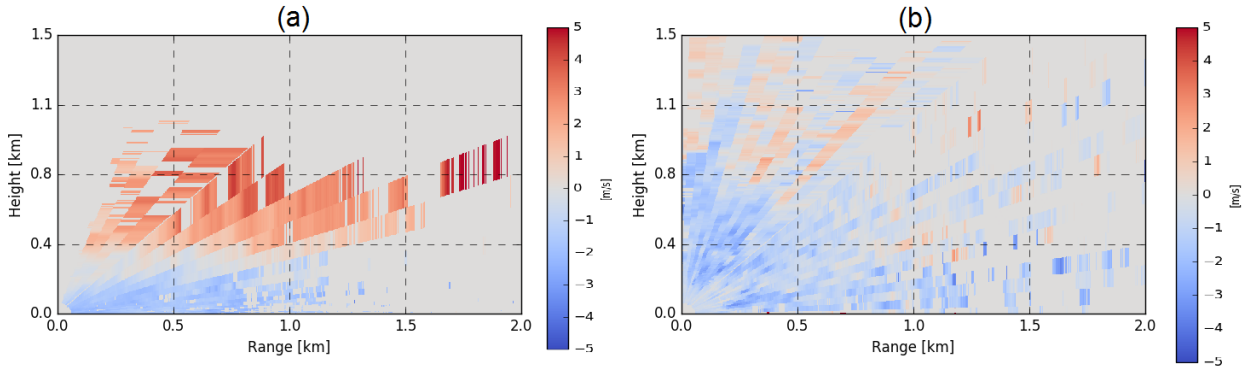

Fig. 13. A snapshot of lidar measurements of radial velocity in ms^{-1} (RHI scan) when the lake-breeze front was passing over (a) Hanlan's Point on 15 July at 1445 UTC (b) Highway 400 ONroute on 9 August at 1815 UTC. Negative (blue) velocities represent winds towards the lidar; positive (red) velocities represent winds away from the lidar. The direction of the x-axis is facing south.

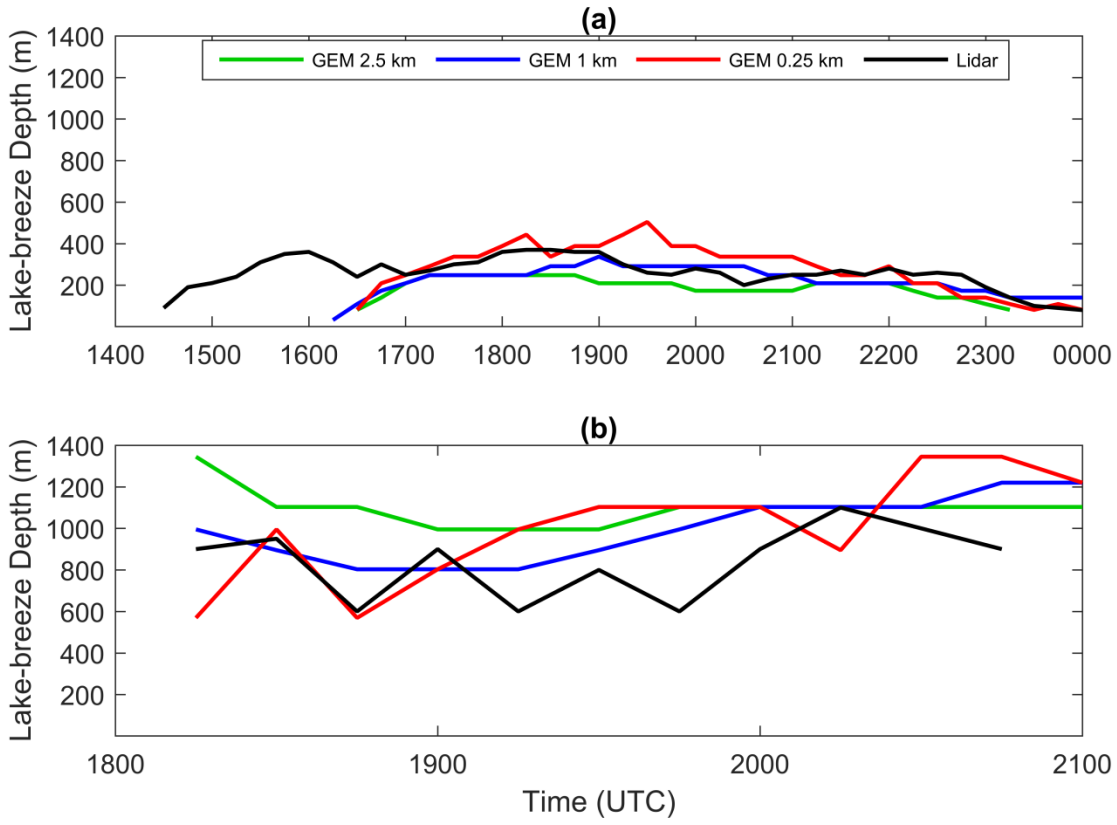

780

781 Fig. 14. Observed and predicted lake-breeze depths using lidar and GEM at intervals of 15
782 minutes at (a) Hanlan's Point on 15 July and (b) Highway 400 ONroute on 9 August. Note that
783 the lake-breeze front arrived at Hanlan's Point and Highway 400 ONroute approximately at 1424
784 UTC and 1815 UTC, respectively. The modeled depths were estimated at the nearest grid point
785 to the lidar sites.

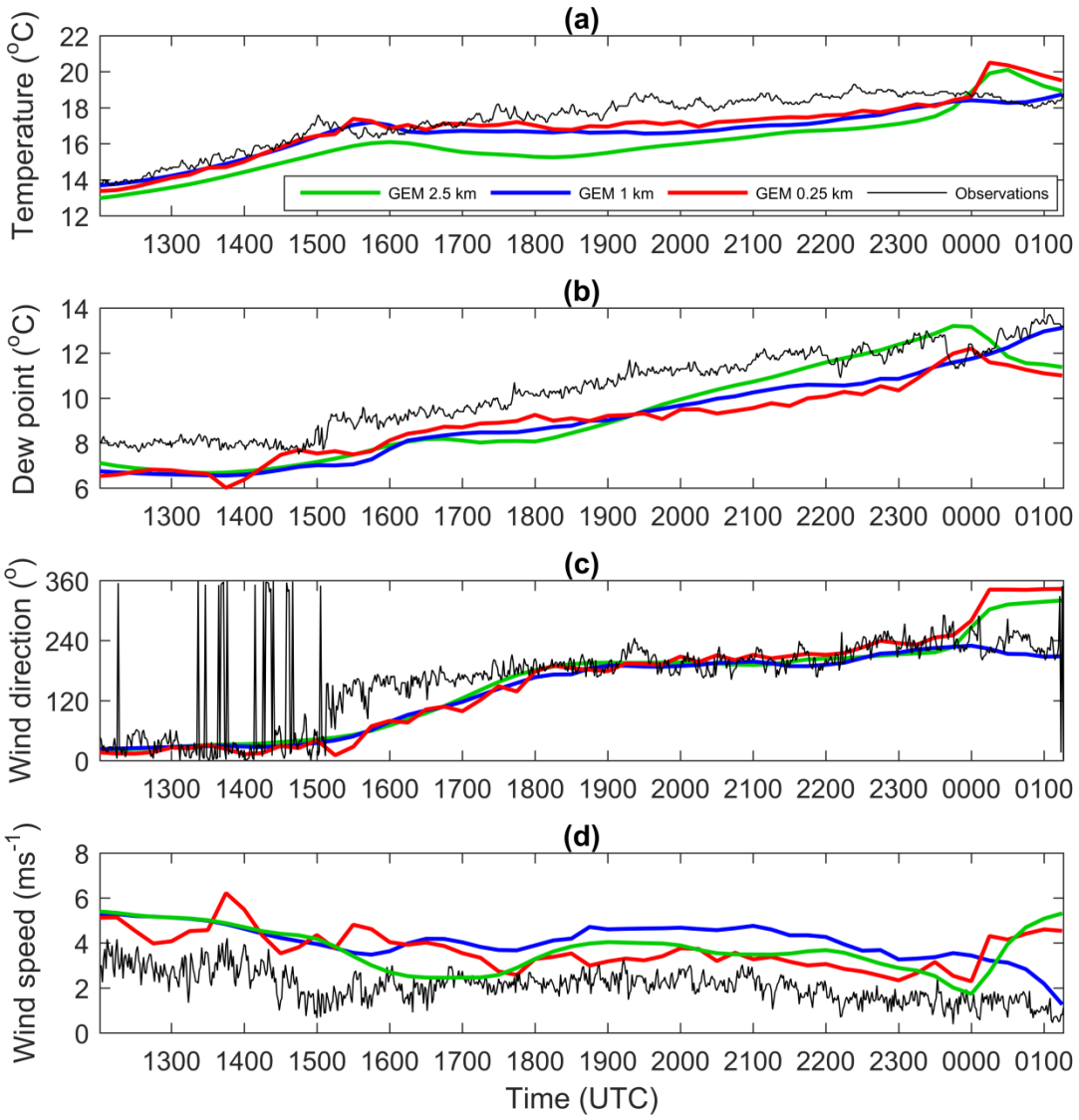

786

787 Fig. 15. Comparisons of observations with the model output at the nearest grid point to Z2D
788 station from the period of 1200 UTC on 15 July to 0115 UTC on 16 July, 2015. (a) temperature
789 (°C), (b) dew point (°C), (c) horizontal wind direction (°) and (d) horizontal wind speed (ms^{-1}).
790 The observed lake-breeze front arrived at 1508 UTC. The temporal resolution of observations
791 and predictions are 1 and 15 minutes, respectively.

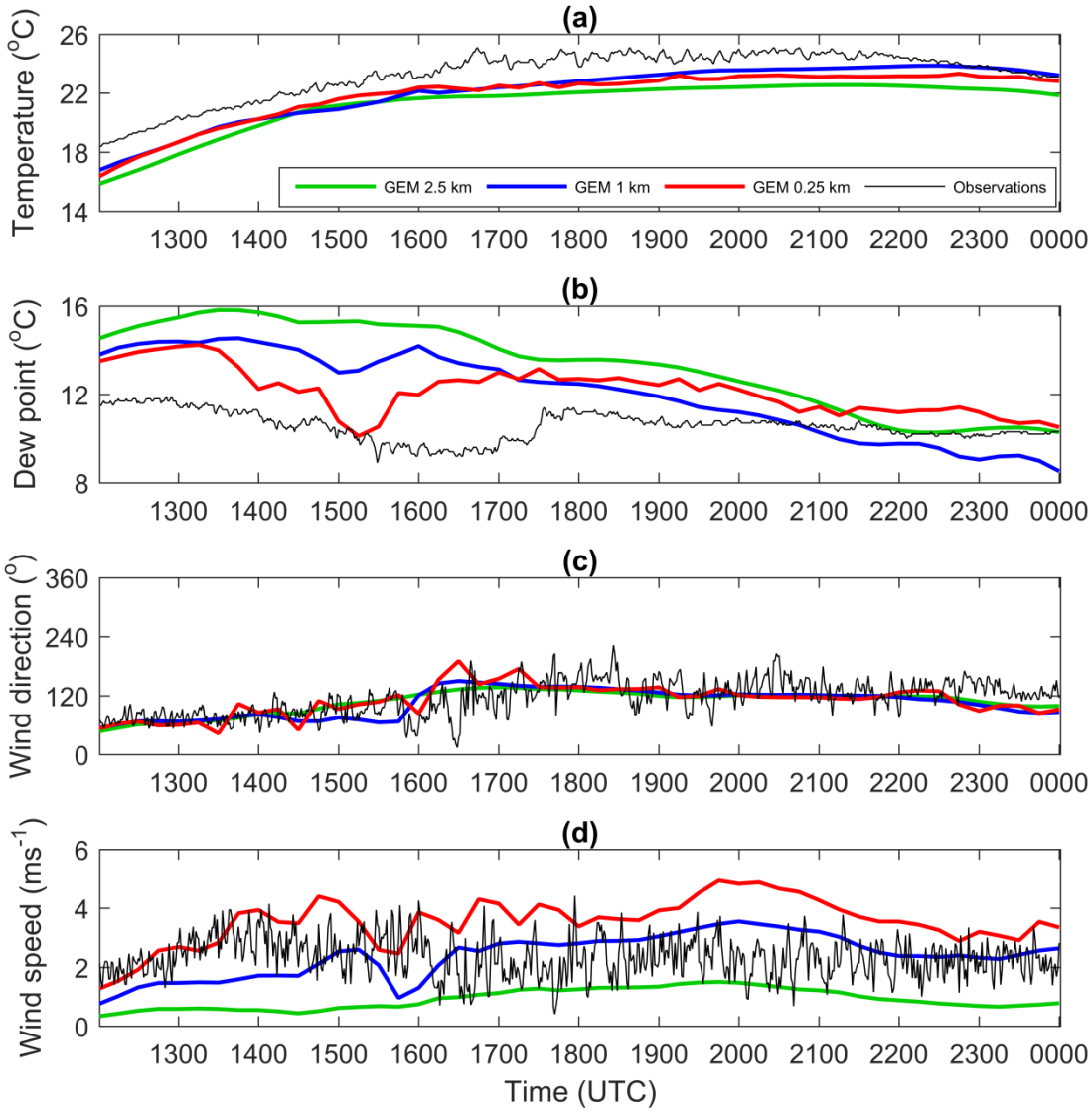

792

793 Fig. 16. The same as Fig. 15 except from 1200 UTC on 9 August to 0000 UTC on 10 August at

794 L1F station. The lake-breeze front arrived at 1643 UTC.

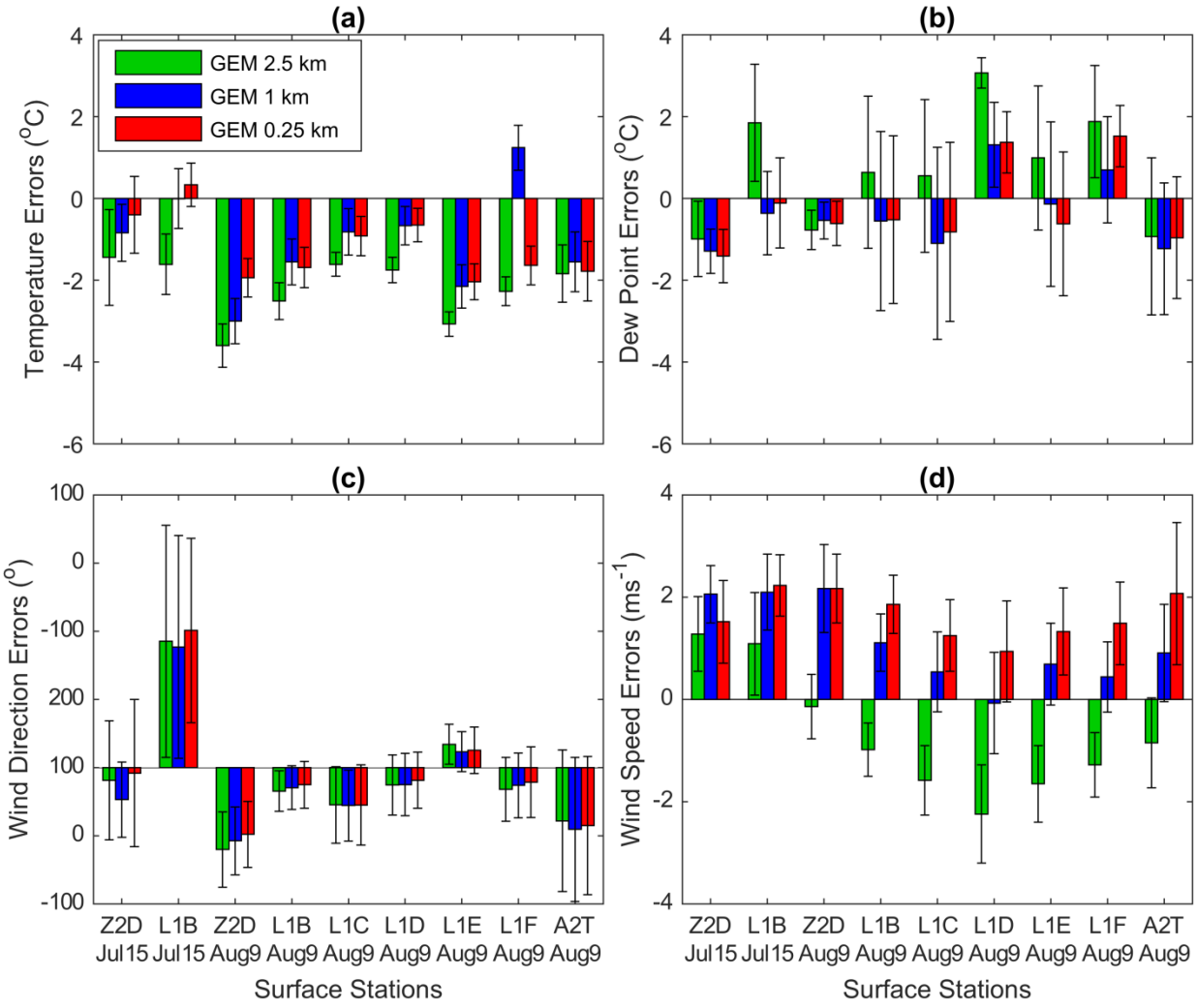

795

796 Fig. 17. The MBE values for (a) temperature (˚C), (b) dew point (˚C), (c) wind direction (˚) and
797 (d) wind speed (ms^{-1}) at the nearest grid point to surface stations for the periods of time that
798 surface stations were affected by the lake-breeze circulations on 15 July and 9 August. The error
799 bars represents the STDE values.

800

801

802

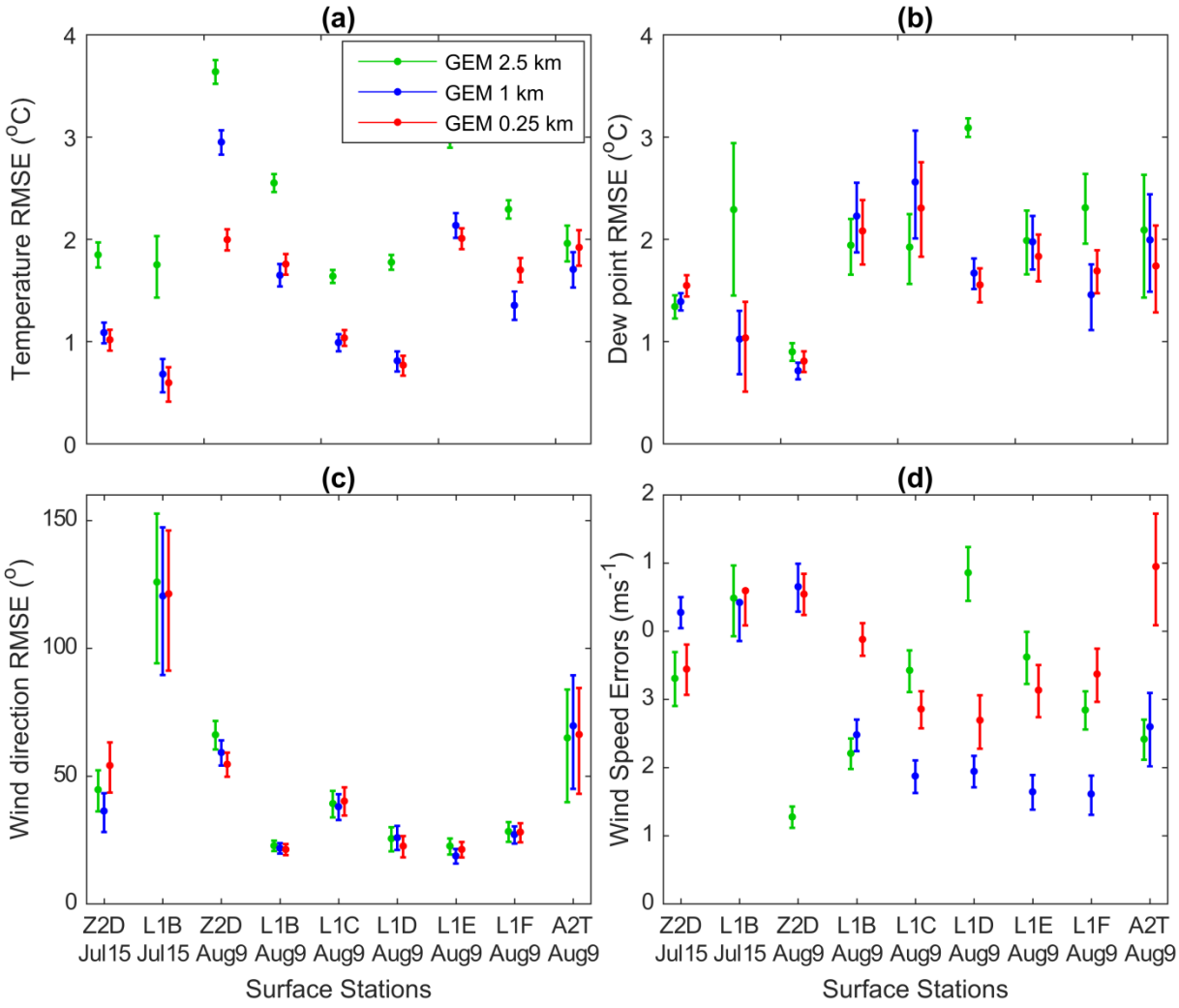

Fig. 18. The RMSE values and corresponding 10% and 90% confidence intervals for (a) temperature (°C), (b) dew point (°C), (c) wind direction (°) and (d) wind speed (ms^{-1}) at the nearest grid point to surface stations for the periods of time that surface sites were affected by the lake-breeze circulations on 15 July and 9 August, 2015.

Appendix A.

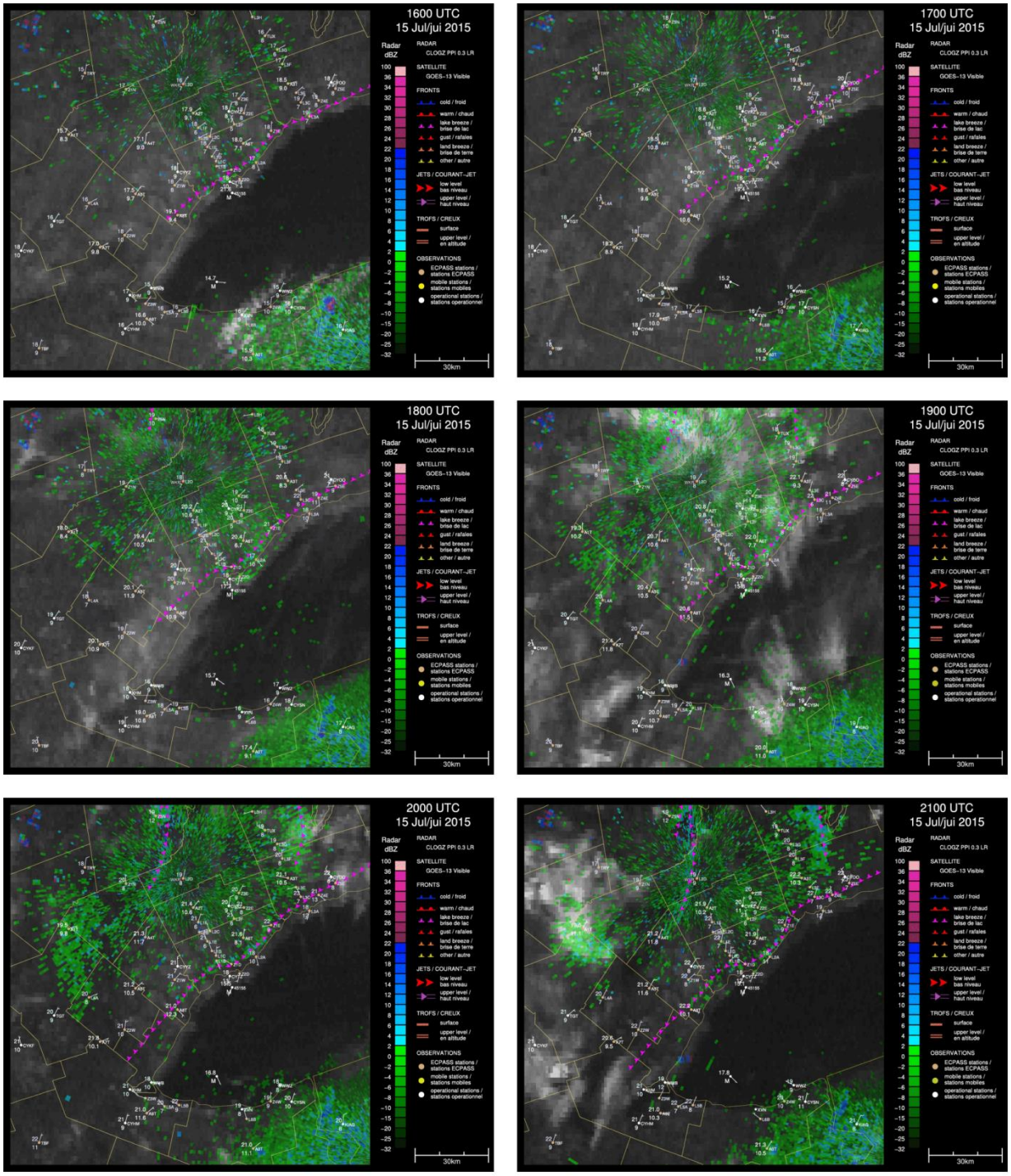

Fig. A1. Hourly mesonet analyses for 15 July, 2015.

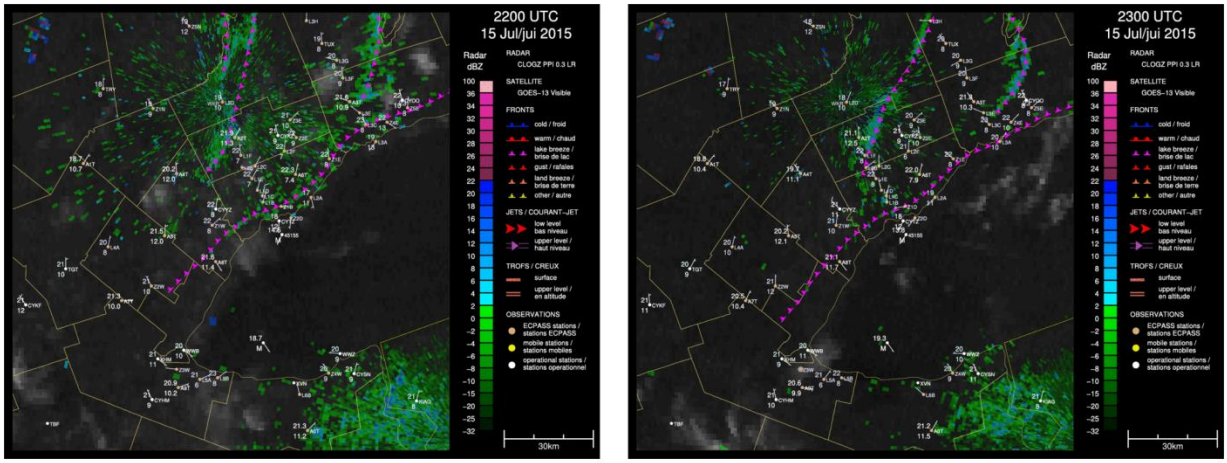

814

815 Fig. A1. (Continued)

816

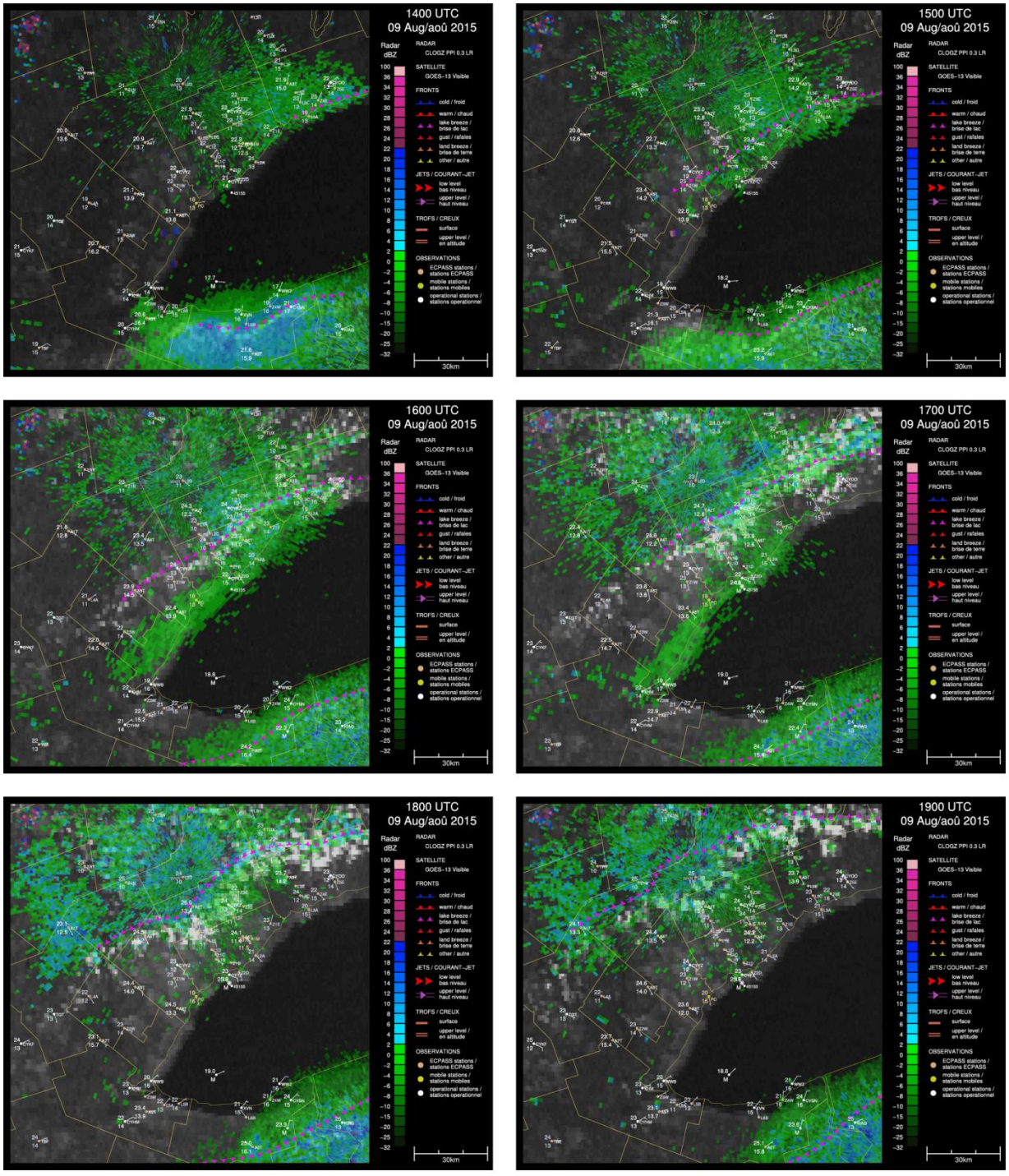

817

818 Fig. A2. The same as Fig. A1 except for 9 August, 2015.

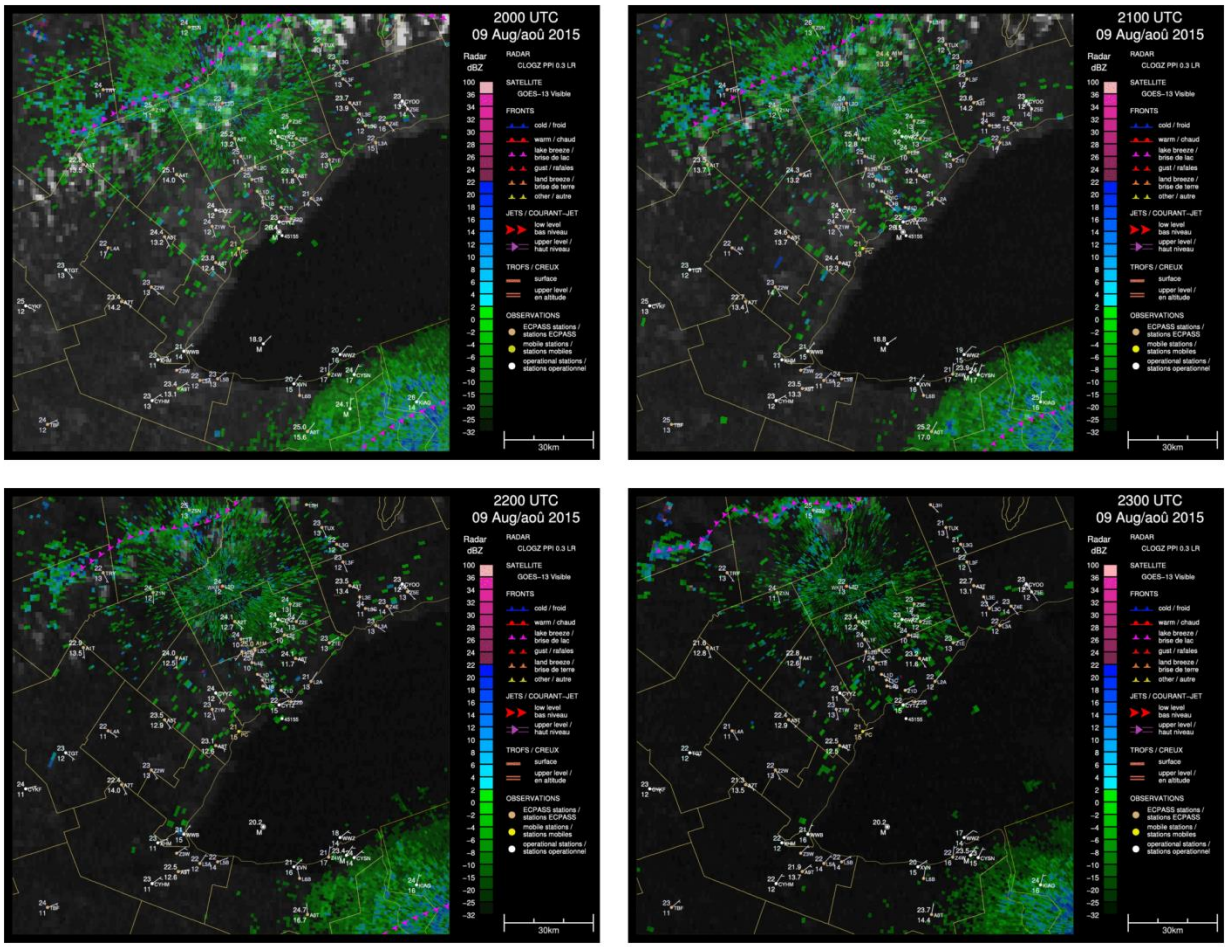

819
820 Fig. A2. (Continued)

821